Australian Government
Department of Defence
Defence Science and
Technology Organisation

Progress Report on Activities in Support of Composite Repair Engineering Development Program Tasks AF, AH and AI

A. N. Rider and D. Parslow

Air Vehicles Division
Defence Science and Technology Organisation

DSTO-TR-1932

ABSTRACT

Research has been undertaken to support the Royal Australian Air Force's commitments to the F/A-18 Composite Repair Engineering Development Program (CREDP). This report details work that has examined the effectiveness of surface treatments for adhesive bonding to aluminium, titanium and stainless steel (Tasks AF and AH) and the benefit of resin injection repairs to damaged composite laminates to restore fatigue strength (Task AI). The studies showed that bonding to high modulus metals using current and new generation surface treatment processes does not appear to be as effective as on aluminium alloys. Resin injection repairs to damaged composite laminates shows some measurable improvements over unrepaired laminates when tested in compression-compression fatigue.

Published by

Air Vehicles Division
DSTO Defence Science and Technology Organisation
506 Lorimer St
Fishermans Bend, Victoria 3207 Australia

Telephone: (03) 9626 7000
Fax: (03) 9626 7999

AR-013-778
November 2006

APPROVED FOR PUBLIC RELEASE

Progress Report on Activities in Support of Composite Repair Engineering Development Program Tasks AF, AH and AI

Executive Summary

The F/A-18 Composite Repair Engineering Development Program (CREDP) has been running since 1984 and provides valuable support for composite and bonded structure maintenance on the Royal Australian Air Force (RAAF) F/A-18 fleet. Participants of the annual international meeting comprise countries currently operating F/A-18 and the purpose of the meeting is to raise issues regarding composite and bonded structure maintenance and develop programs to solve these problems. The programs are undertaken through a cooperative agreement in which each of the partner nations completes various activities that contribute to an overall task. Currently, Air Vehicles Division (AVD) from the Defence Science and Technology Organisation (DSTO) is providing technical support to meet RAAF's CREDP obligations in a number of active CREDP tasks.

The following report details experimental results that are contributing to the CREDP tasks. The tasks included the following: Task AI- Fatigue Testing of Injected Coupons, Task AF-Metal Bonding for Repair: Phase II and Task AH-Metal Bonding for Repair: Phase III. The objective of Task AI was to establish if resin injection repairs of impact-damaged composites were effective in restoring the fatigue durability of the composite laminate. Task AF was primarily concerned with establishing if the clad layer on Al7075 aluminium alloy would compromise the environmental and/or fatigue durability of the adhesively-bonded joints formed with FM300-2K adhesive. The focus of Task AH was to establish the effectiveness of a range of different surface treatments being used by the different partner nations for adhesive bonding to metallic substrates, particularly steel and titanium alloys.

Results from wedge testing suggest that the durability of adhesive bonds was clearly reduced on the high modulus alloys, such as Ti-6Al-4V, PH13-8Mo and 301 stainless steel, when compared to Al7075-T76 alloys. Some previous research at DSTO has suggested that the current grit blast and silane process can be improved on titanium alloys if the abrasion step is removed prior to grit blasting. As both epoxy silane and sol-gel treatments faired equally poorly on the Ti 6Al-4V, it may be that abrasion is reducing the effectiveness of the sol-gel treatment also.

Compression-compression fatigue testing on damaged and resin injection repaired composite laminates suggested that some recovery in performance resulted with the injection repair. The extent of the improvement was not easily quantifiable; however, repaired laminates exhibited average failure stresses in compression fatigue similar to those observed for undamaged baseline laminates.

Authors

Andrew Rider
Air Vehicles Division

Andrew Rider has been employed by Air Vehicles Division since 1989 and has been involved in research examining surface treatments for bonded repairs to composite and metallic substrates. He is currently involved in the development of materials and processes for repairs to current and new generation aircraft.

David Parslow
Air Vehicles Division

David Parslow is a senior technician working with Air Vehicles Division. David has extensive experience and expertise in the operation of static and dynamic fatigue machines and has testing experience with a wide range of metallic and composite material systems.

Contents

1. Introduction

The F/A-18 Composite Repair Engineering Development Program (CREDP) has been running since 1984 and provides valuable support for composite and bonded structure maintenance on the Royal Australian Air Force (RAAF) F/A-18 fleet. Participants of the annual international meeting comprise countries currently operating F/A-18 and the purpose of the meeting is to raise issues regarding composite and bonded structure maintenance and develop programs to solve these problems. The programs are undertaken through a cooperative agreement in which each of the partner nations completes various activities that contribute to an overall task. Currently, Air Vehicles Division (AVD) from the Defence Science and Technology Organisation (DSTO) is providing technical support to meet RAAF's CREDP obligations in a number of active CREDP tasks.

The following report details experimental results that are contributing to the CREDP tasks. The tasks included the following: Task AI- Fatigue Testing of Injected Coupons, Task AF-Metal Bonding for Repair: Phase II and Task AH-Metal Bonding for Repair: Phase III. The objective of Task AI was to establish if resin injection repairs of impact-damaged composites were effective in restoring the fatigue durability of the composite laminate. Task AF was primarily concerned with establishing if the clad layer on Al7075 aluminium alloy would compromise the environmental and/or fatigue durability of the adhesively-bonded joints formed with FM300-2K adhesive. The focus of Task AH is to establish the effectiveness of a range of different surface treatments being used by the different partner nations for adhesive bonding to metallic substrates, particularly steel and titanium alloys.

2. Task AF -Metal Bonding for Repair: Phase II

2.1 Experimental

The objectives of Task AF were to evaluate the effectiveness of the field level sol-gel process [1], [2] and the grit blast and epoxy silane treatment [3]with and without primer on 7075-T76 aluminium during bonding and to compare the effectiveness of bonding processes of either removing or retaining cladding. DSTO was asked to complete and test the wedge test specimens [4] detailed in Table 1. All specimens were bonded with FM300-2K in accordance with SRM 250 and were tested at 50°C/95% R. H. for nine days. Pass and failure was based on less than 0.2 ” (5 mm) and 0.25 “ (6.35 mm) crack growth over a 24- and 48-hour period, respectively. Additionally, 95% or more cohesion failure in the cracking zone was required. Details of the grit blast and silane treatment are provided in Appendix A.1.

Table 1 Wedge test matrix for DSTO's contribution to CREDP Task AF

Designation	Aluminium Alloy	Surface Preparation
GBSP 7075T76UC	Bare 7075-T76	Scotchbrite abrade, solvent clean, grit-blast, 1% aqueous epoxy silane, BR-127 prime
GBSNP 7075T76UC	Bare 7075-T76	Scotchbrite abrade, solvent clean, grit-blast, 1% aqueous epoxy silane
GBSP 7075T6C	Clad 7075-T76	Scotchbrite abrade, solvent clean, grit-blast, 1% aqueous epoxy silane, BR-127 prime

2.2 Results

The individual measurements for the five test pieces for each treatment in Table 1 are provided in Appendix A.2. The fracture toughness values, G_I (J/m^2), were calculated using equation 1.

$$G_I = \frac{Y^2.E.h^3\left[3\left(a+0.6h\right)^2+h^2\right)\right]}{16\left[\left(a+0.6.h\right)^3+a.h^2\right]^2} \qquad (1)$$

where Y is the crack opening displacement, h is the adherend thickness, E is Young's modulus (72.4 GPa for Al-7075) and a is crack length. Both the crack length and fracture toughness as a function of square root time are shown in Figure 1 and 2, respectively.

The level of cohesive failure for each treatment is shown in Table 2 and the images of the failure surfaces are provided in Appendix A.3.

Table 2 Cohesive failure percentages for the Al7075 wedge test samples bonded with grit-blast and silane treatment.

Specimen	Cohesive Failure (%)					
	1	2	3	4	5	Average
GBSP 7075T76UC	100	85	90	90	95	92.0
GBSNP 7075T76UC	94	94	98	100	100	97.2
GBSP 7075T6C	30	40	50	35	20	35

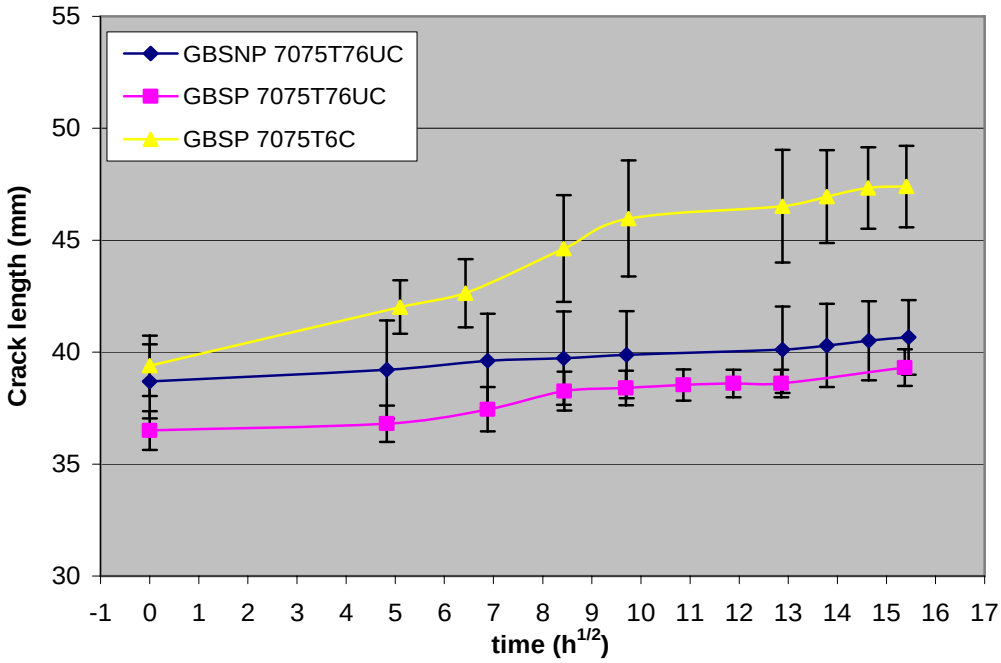

Figure 1 Crack length as a function of square root time for Al7075-T76 and Al7075-T6 treated with the grit blast and silane treatments.

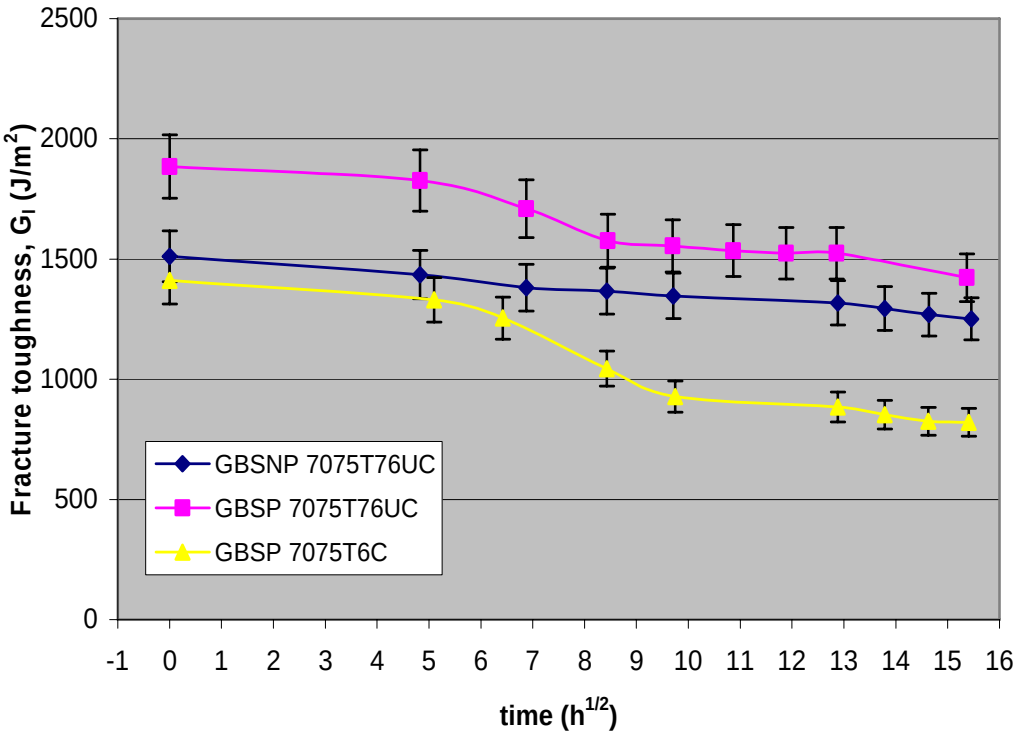

Figure 2 Fracture toughness (G_I) as a function of square root time for Al7075-T76 and Al7075-T6 treated with the grit blast and silane treatments.

2.3 Discussion

The bond durability of the grit blast and epoxy-silane-treated Al7075-T76 samples are relatively similar based on the final crack length and fracture toughness values after nine days humid exposure. The treatment without primer performs slightly better than the primed surface and this is also reflected in the increased level of cohesion failure observed (Table 2). Images of the failure surfaces (Appendix A.3) clearly show that the primed surface has more adhesion failure at the FM300-2K and metal interface. Based on the pass and failure criteria of less than 0.2 ” (5 mm) and 0.25 “ (6.35 mm) crack growth over a 24- and 48-hour period, respectively, both samples would pass. However, the additional requirement that no samples should exhibit less than 95% cohesion failure means that neither sample would pass.

One of the difficulties that arises with visual observation of failure mode in the cracking zone is for cases where samples exhibit high levels of voiding. In the case of both the primed and unprimed Al7075-T76 samples, it is clear in Appendix A.3 that both specimens have voiding. It would seem unlikely that in either case the crack would have propagated interfacially as the crack growth is between 2 mm to 3 mm and is likely to be due to adhesive creep. This may need consideration as to basis on which samples are failed, i.e. poor surface treatment or high bondline voiding.

Unlike the Al7075-T76 samples, the Al7075-T6 clad aluminium sample treated with grit blast, silane and primer showed significantly poorer durability. The sample would fail the criteria on the basis that very low levels of cohesion failure were observed in the cracking zone. Despite the clearly poorer performance, the wedge sample would have passed on the basis of crack growth in the 24- and 48-hour periods. Images of the clad Al7075-T6 wedge samples in Appendix A.3 clearly exhibit high levels of interfacial failure, suggesting the grit blast, silane and primer surface treatment is clearly inferior on the clad alloy surface.

The relative performance of the three samples over a three-day period of exposure raises clear questions over the criteria that should be used in a pass/fail quality control environment to ensure bond quality. Whilst a 48-hour test offers clear advantages in time, it is clear that increased exposure times may lead to significant deterioration in bonds that may initially have been considered adequate. It is evident that the combination of prescribed crack growth limits and failure mode are both required to adequately qualify bond quality and both elements are critical if shorter test times are to be used.

2.4 Conclusions

1) Grit blast and silane with and without BR127 primer surface treatment provides a durable adhesive bond with FM300-2K on Al 7075-T76 alloy as determined by wedge test crack growth over 48 hours in a 50°C/95% R.H. environment.
2) Grit blast and silane with BR127 primer surface treatment for bonding FM300-2K to clad Al 7075-T6 alloy would not pass the current RAAF criteria based on high levels of adhesion failure in the cracking zone over a 48-hour period in a 50°C/95% R. H. environment.

3. Task AH -Metal Bonding for Repair: Phase III

3.1 Experimental

The main purpose of Task AH was to extend the application of current surface treatments to high elastic modulus materials including titanium and steel alloys. The higher modulus materials may be either found on F/A-18 structure or used as patch materials where thinner repairs are required. The main objectives of the task were to: 1) evaluate the effectiveness of the field level sol-gel surface treatment with and without primer on titanium alloys, and 2) test depot level sol-gel treatment and grit blast and silane treatment on Ti 6Al-4V, 301 and PH13-8Mo stainless steels. DSTO was asked to complete and test the wedge test specimens detailed in Table 3. All specimens were bonded with FM300-2K in accordance with SRM 250 and were tested at 50°C/95% R. H. for nine days. Pass and failure was as detailed in section 2.1. Details of the sol-gel treatment are provided in Appendix B.1 and images of the corresponding failure surfaces are shown in Appendix B.3.

Table 3 Wedge test matrix for DSTO's contribution to CREDP Task AF

Designation	Aluminium Alloy	Surface Preparation
GBSP Ti6-4	Ti-6Al-4V	Scotchbrite abrade, solvent clean, grit-blast, 1% aqueous epoxy silane, BR-127 prime
GBGNP Ti6-4	Ti-6Al-4V	Scotchbrite abrade, solvent clean, grit-blast, sol-gel
GBGNP 301SS	301 Stainless Steel	Scotchbrite abrade, solvent clean, grit-blast, sol-gel
GBGNP PH13-8Mo	PH13-8Mo	Scotchbrite abrade, solvent clean, grit-blast, sol-gel

3.2 Results

Both the crack length and fracture toughness as a function of square root time are shown in Figures 3 and 4, respectively, for the surface treatments detailed in Table 3. Fracture toughness was calculated using equation 1. The modulus values used for the G_I calculations were 113.8 GPa, 212 GPa and 230 GPa for the Ti-6Al-4V, 301 stainless steel and PH13-8Mo, respectively. The individual data measured for each test is provided in Appendix B.2. The percentage of cohesion failure for each wedge test is shown in Table 4 and images of the failure surfaces are shown in Appendix B.3.

Table 4 Cohesive failure percentages for the titanium and steel wedge test samples bonded with the sol-gel and grit-blast and silane treatments

Specimen	Cohesive Failure (%)					
	1	2	3	4	5	Average
GBSP Ti6-4	30	5	3	35	20	18.6
GBGNP Ti6-4	5	45	25	20	1	19.2
GBGNP 301SS	50	50	35	10	50	39.0
GBGNP PH13-8Mo	35	35	40	20	40	33.7

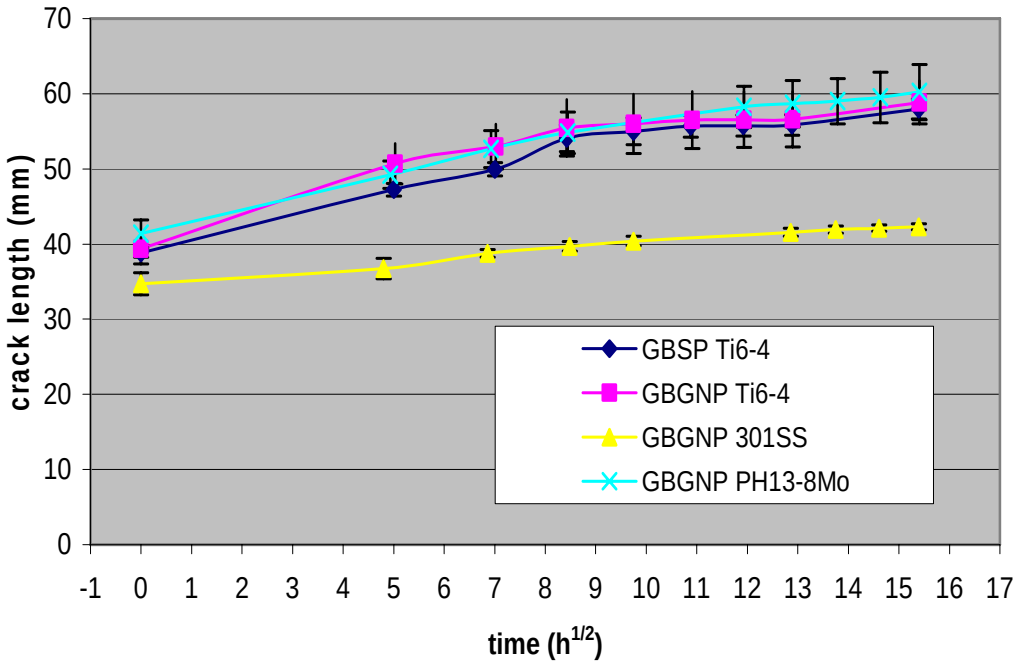

Figure 3 Crack length as a function of square root time for titanium and steel treated with sol-gel and the grit blast and silane treatments

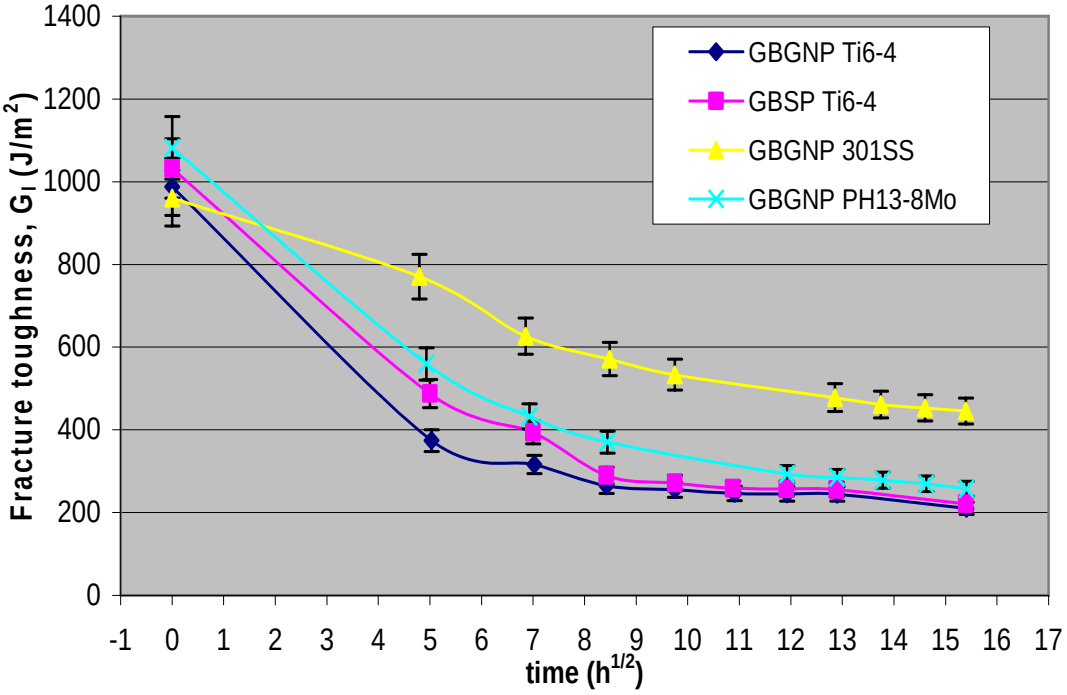

Figure 4 Fracture toughness (G_I) as a function of square root time for titanium and steel treated with sol-gel and the grit blast and silane treatments

3.3 Discussion

The performance of the wedge tests made from titanium and steel is clearly inferior to the aluminium wedge test specimens. The 301 stainless steel sample, whilst being clearly better than the titanium and PH13-8Mo samples, is still inferior to any of the 7075 alloy specimens. All samples would have failed the criteria detailed in section 2.1. This suggests that both the sol-gel and epoxy silane treatments may not be as effective and that procedures that include primers that are optimised for FM300-2K may need to be examined. Previous work by DSTO that examined the grit blast and silane treatment on Ti-6Al-4V also suggested poorer performance relative to aluminium [5]. Table 5 shows the results from the previous DSTO work. It is clear that the values around 200 J/m^2 after nine hours for the titanium substrates compares well with the value between 150 and 200 J/m^2 after 1,000 hours humid exposure in the previous work.

Table 5 Wedge test results from previous DSTO testing of the grit blast and silane treatment on Ti 6Al-4V and FM300-2K adhesive [5]

Treatment	**G_I (J/m^2) at 0 hours exposure**	**G_I (J/m^2) at 1000 hours exposure**
Grit-blast and epoxy silane (GBSNP)	1190	205
Grit-blast and epoxy silane and BR127 primer (GBSP)	1141	155

Additional research since 2002 on bonding to titanium has suggested that the abrasion processes leave embedded particles in the surface layer that are not easily removed with tissue wiping, but which form a weak boundary layer on the metal surface through which fracture can propagate. This is demonstrated by surface analysis studies that have been used to characterise the abraded and grit-blasted titanium surfaces before bonding and after wedge test fracture. Figure 5 shows that silicon from the Scotchbrite® abrasion pad peaks around 12 atomic percent and then decreases slowly with depth. In contrast, the grit-blasted surface shows a much lower level of silicon from the coupling agent that drops to zero quickly. This indicates that the abrasion has left embedded particles from the scouring pad embedded in the titanium surface. Interestingly, the grit blasting leaves a surface in which high levels of alumina grit have been left embedded in the surface of the titanium. Table 6 shows that high levels of silica are observed in all the fracture surfaces, which exposed the FM300 adhesive surface. This provides some evidence that the embedded particles from abrasion are being pulled out of the titanium surface during fracture.

Based on some of the evidence described, that the embedded particles from abrasion were providing a weak boundary layer for fracture, some subsequent surface treatment development on high modulus PH 17-7 stainless steel in the TH1050 condition removed the abrasion step from the grit blast and silane process [6]. The results of crack length and fracture toughness for unclad Al2024-T3 and the PH 17-7 stainless steel are shown in Figure 6. The stainless steel was 2.2 mm (0.0865 ″) thick and the wedge was 3 mm (0.118 ″) thick. It can be seen after 48 hours that the fracture toughness values are comparable for the stainless steel and aluminium wedge samples. These results provide some confidence that the removal of the abrasion step can improve the surface treatment performance.

Clearly, similar experiments are required on other high modulus steels and titanium alloys to establish if other factors are also contributing to overall performance.

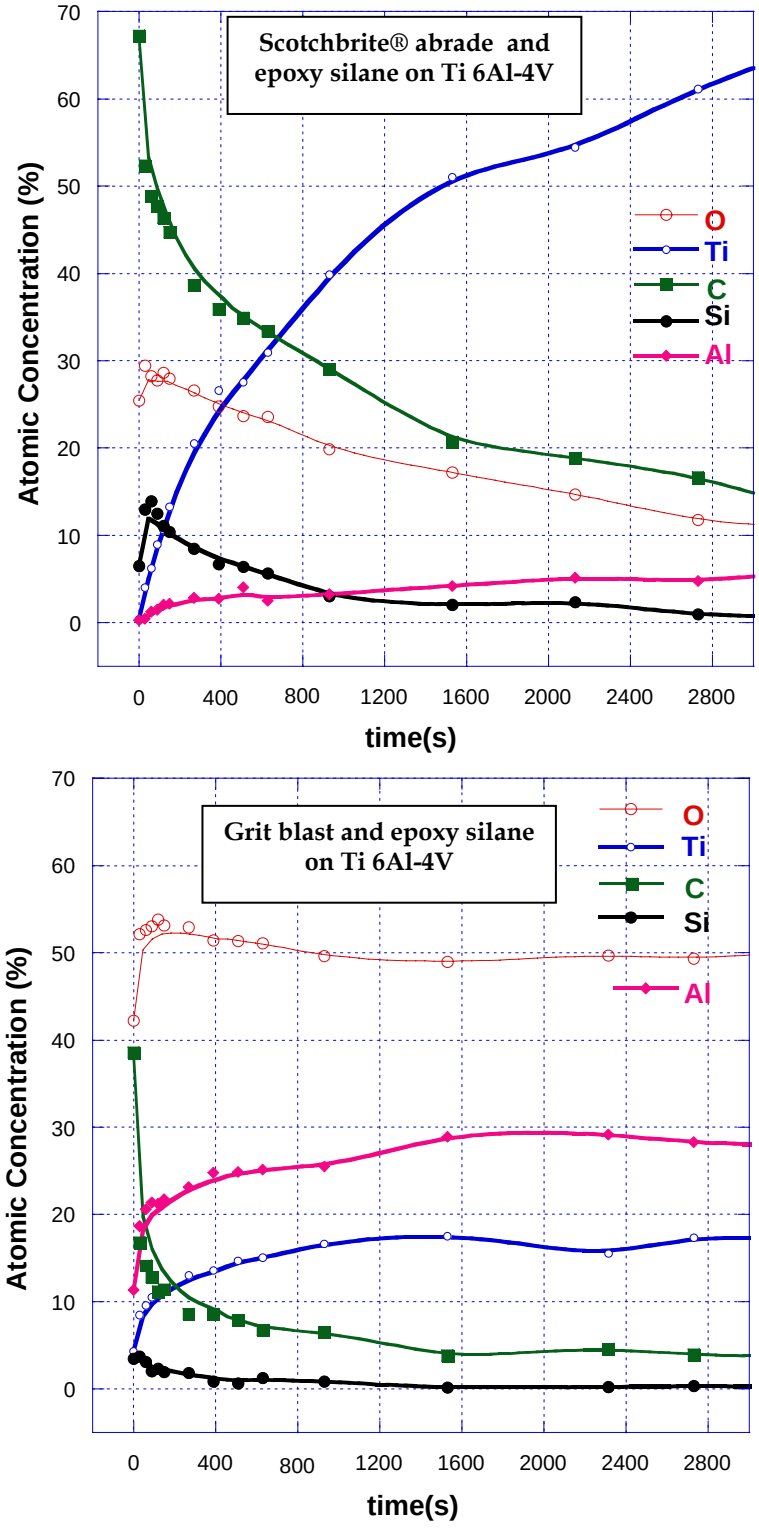

Figure 5 Atomic concentration as a function of ion milling time for Ti 6Al-4V Scotchbrite® abraded and grit-blasted surfaces treated with 1% aqueous epoxy silane solution

Table 6 Atomic concentrations of wedge test failure surfaces in which Ti 6Al-4V was bonded to FM300 adhesive

Sample	Side	Atomic Concentration (%)								
		C1s	O1s	Ti2p	Si2s	Al2p	N1s	Na1s	Sr3d	Cr2p
Scotchbrite abrade + silane	Adhesive	53.1	31.5	0.6	8.3	1.9	1.8	2.8	---	---
	Metal	33.4	41.8	14.7	2.4	---	0.7	7.0	---	---
Grit-blast + silane	Adhesive	51.5	34.1	0.4	4.9	1.7	2.9	4.6	---	---
	Metal	45.8	36.7	2.6	2.5	4.7	3.5	4.3	---	---
Grit-blast + silane + BR127	Adhesive	51.0	34.5	0.4	5.7	1.4	2.4	2.4	0.3	1.9
	Metal	41.3	35.7	1.5	4.4	7.6	2.4	2.0	1.0	4.2

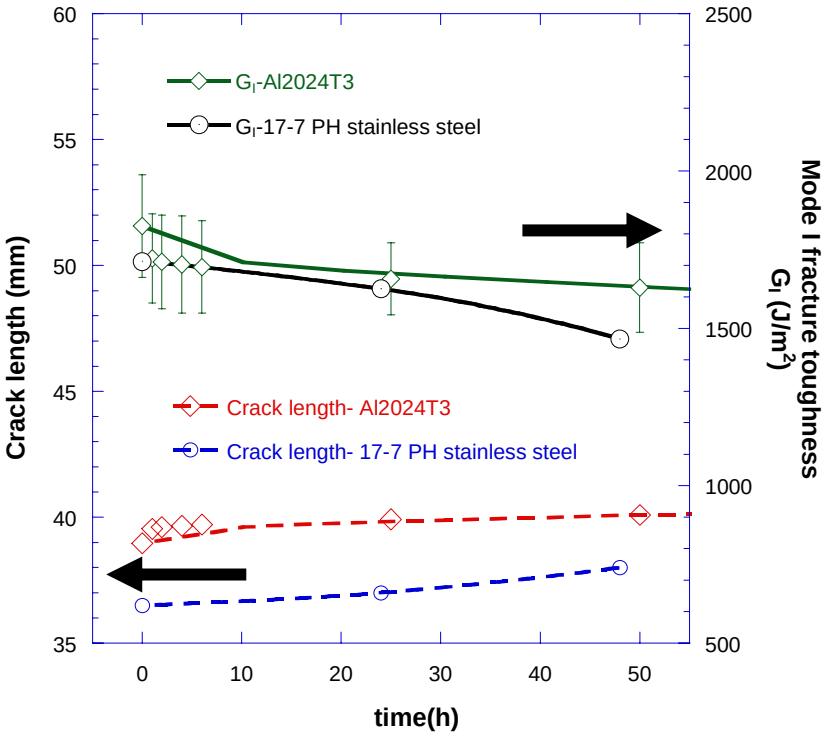

Figure 6 Comparison of crack length and fracture toughness, G_I, for bare aluminium Al2024-T3 and PH 17-7 stainless steel in the TH1050 condition pretreated using the grit-blast and silane method and bonded with FM300

3.4 Conclusions

1) Current surface treatments using grit blast and silane with and without BR127 primer do not pass the criteria stipulated in AAP 7021.016-2 when bonding to Ti 6Al -4V, 303 stainless steel or PH13-8 Mo.
2) Current surface treatments using grit blast and sol-gel without primer do not pass the criteria stipulated in AAP 7021.016-2 when bonding to Ti 6Al -4V, 303 stainless steel or PH13-8 Mo.

3) Removal of the abrasion process may improve surface treatment performance on high modulus steels by preventing fracture through a weak boundary layer of weakly embedded particles.

4. Task AI-Fatigue Testing of Injected Coupons (Task T-Phase II)

4.1 Background

The low interlaminar shear strength of composites makes them prone to damage from relatively low-impact energy. The low interlaminar shear strength means impact damage can lead to delamination and/or fibre breakage. As a consequence, the compression strength and strain to failure may be significantly reduced. Task AI investigated novel injection repair techniques in an attempt to recover the interlaminar shear strength of impact-damaged composites. There is quite a deal of debate over the effectiveness of resin injection repairs and the objectives of Task AI were to: 1) redesign a resin injection repair device (RID) to improve the efficiency of the repair process, 2) practically apply the RID on damaged composite laminates, and 3) evaluate the extent of structural restoration of the panels. Full details of the process for producing the resin injection repaired composite laminates are provided in reference [7].

4.2 Experimental

Briefly, composite laminates were prepared to reflect the structures and delaminations that occur on F/A-18 doors 79 and 143. The 32-ply laminates (Figure 7) were manufactured by Bombardier from 0.0052" thick Hercules AS4/3501-6 carbon/epoxy unidirectional prepreg with the stacking sequence $[45/0/-45/90]_{4s}$. Resin injection repair used the device shown in Figure 8 with EA9396 from Loctite.

Delaminations were created by using the jig shown in Figure 9. Loading was applied through the stainless steel ball until a sudden drop was recorded. The size of the delamination was controlled by adjusting the support diameter. Damage with diameters from 2 to 4 " was produced. C-scan images were used to measure the delamination diameter before and after injection repair.

Specimens received at DSTO were cut to 7 " by 7 " dimensions before testing. Samples were tested using the Suppliers Advanced Composite Materials Association (SACMA) Compression After Impact (CAI) method [8]. The compression-compression fatigue life of the composite laminates was tested using a 250 kN hydraulically-driven Instron using MTS basic test ware. Samples were tested using a R ratio of 0.1 and a frequency of 5 Hz. The stress was determined by measuring the gross section thickness across the width of the sample, ignoring the countersunk hole area. Initial samples were tested at set maximum stresses, e.g. σ_{max}=120 MPa and σ_{min}=12.0 MPa, until failure was observed. Unfortunately, due to large scatter in cycles to failure for a set σ_{max} it was decided to

fatigue specimens for 100,000 cycles at each load increment. Samples were fatigued 100,000 cycles at a starting stress between 120 and 160 MPa. The load was then incremented in 10 MPa steps and cycled for a further 100,000 cycles. The process was repeated until failure resulted. Hence, it was decided that if the specimen could sustain 100,000 cycles at a set load, fatigue failure was unlikely to occur for that stress level. Whilst this does not provide an idealised S-N curve, the scatter in the composite fatigue durability measured for the initial samples would require a very large data set to produce any meaningful results in the traditional manner.

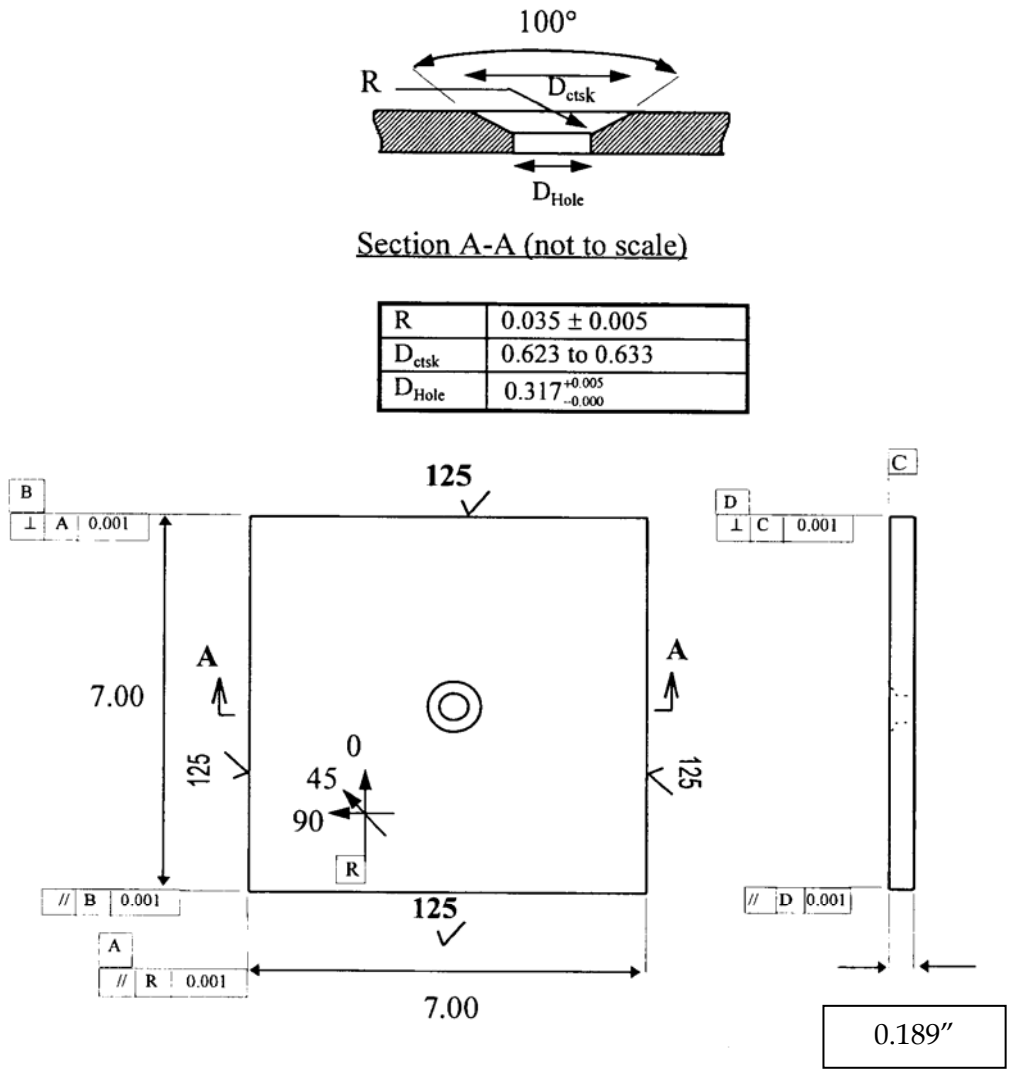

Figure 7 Dimensions of the composite laminates used in the injection repair studies, showing the dimensions and location of the countersunk hole [7]

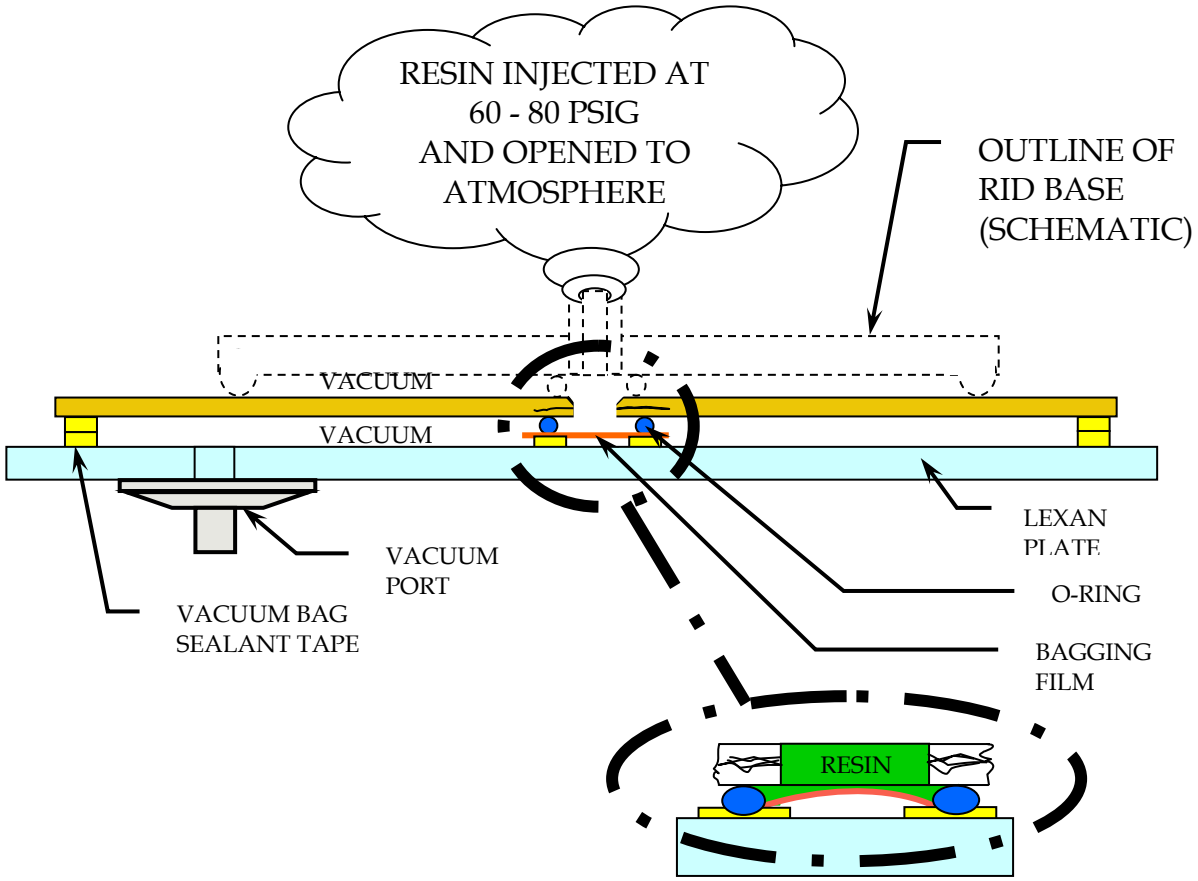

Figure 8 Resin injection device used by Bombardier to repair damaged composite panels [7]

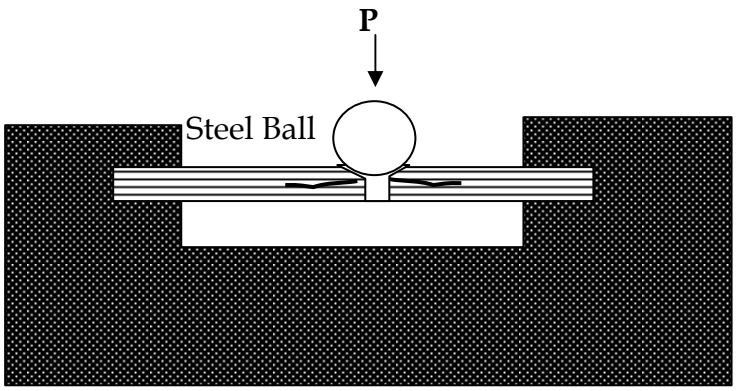

Figure 9 Schematic representation of the jig used to create the delaminations

4.3 Results

Table 7 shows the laminates manufactured at Bombardier: the baseline laminates without damage, the laminates with controlled delaminations and the delaminated samples that were repaired with resin injection. The compression-compression fatigue performance of the laminates described in Table 7 is shown in Figure 10. Full results are provided in Appendix C. Open symbols represent stress levels for which no failure was recorded,

whereas filled symbols show the stress values for which failure occurred. The results can generally be grouped into two areas. The baseline laminates and the repaired laminates appear to have relatively similar performance, although the baseline laminates exhibit some higher stress levels for which failure occurred compared with the repaired laminates. The damaged laminates all appear to have failure stresses below those measured for the baseline and repaired laminates. Interestingly, the only repaired laminate that fails in the same area as the damaged laminates occurred for a sample that was identified as not having been successfully injected.

The statistical significance of the results is not clearly gauged, however, there does appear to be a difference between the repaired and damaged samples, particularly the amount of scatter. The damaged samples show quite a stress range over which fatigue failure was observed - between 130 and 170 MPa. The majority of repaired samples fail around 180 MPa. The variability in the failure stresses recorded for the damaged samples may be partly related to the delamination size. Figure 11 shows the maximum failure stress corresponding to the delamination area. For the damaged samples, the correlation between the failure stress and damaged area is weak, with some suggestion lower failure stresses correspond to larger delamination areas. The repaired samples show that the repair areas are not as spread as the damaged samples, with results clustered around 180 MPa.

Table 7 Composite specimens manufactured to examine the compression-compression fatigue of baseline, damaged and injection repaired laminates

Panel No.	Delamination Diameter (in.)	Comment
1.14	None	Baseline Coupons
1.15		
1.19		
2.6		
2.10		
2.12		
3.7		
3.13		
3.18		
1.16	3.9	Samples delaminated using jig shown in Figure 9
1.18	2.7	
2.7	3.1	
2.8	3.9	
2.16	3.5	
3.3	4.5	
3.10	3.1	
3.15	3.6	
3.17	3.8	
1.1	3.1	Injection Repair OK
1.2	2.7	Injection Repair Poor
1.3	3.0	Injection Repair OK
1.5	2.8	Injection Repair OK
1.6	2.6	Injection Repair OK
1.7	2.7	Injection Repair OK
1.20	3.9	Injection Repair Poor
2.19	3.4	Injection Repair Partially successful
2.20	3.1	Injection Repair OK

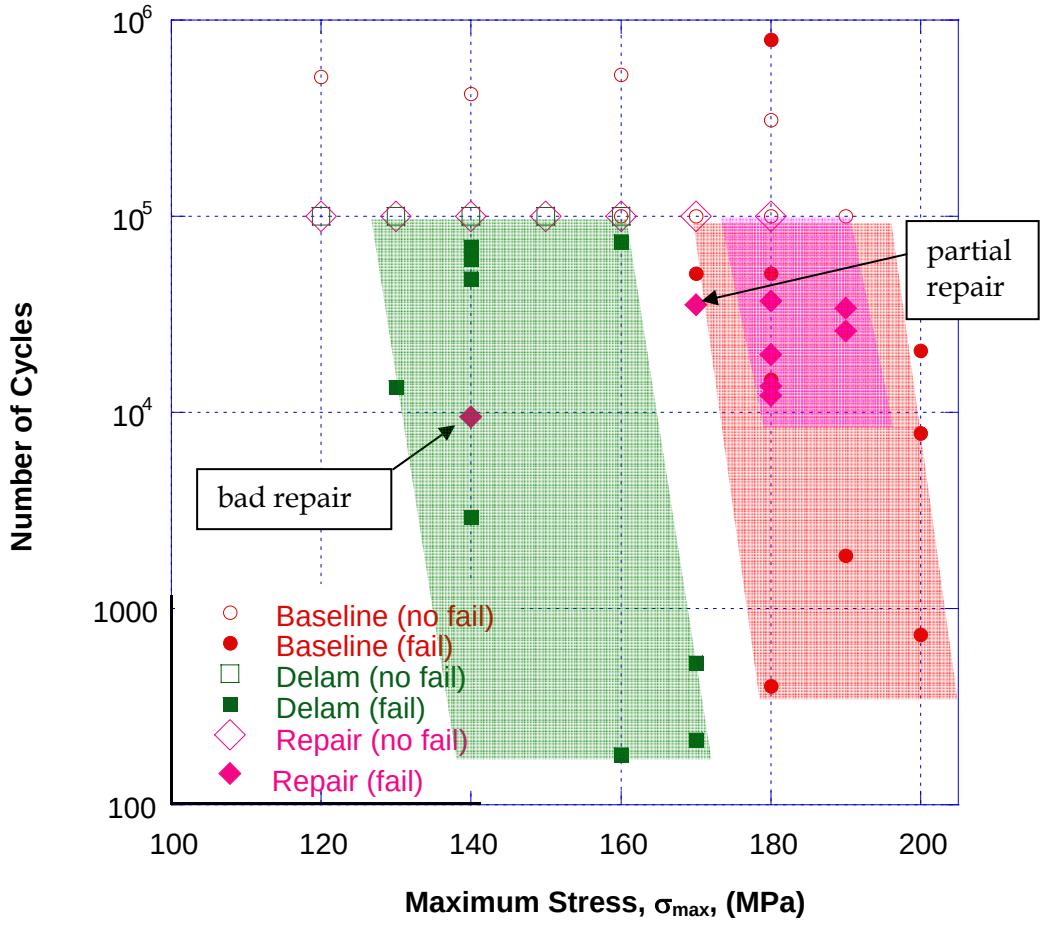

Figure 10 Number of compression-compression fatigue cycles as a function of σ_{max} for the three types of composite laminates: baseline (red), delaminated (green) and repaired (pink). Failure is designated by filled symbols

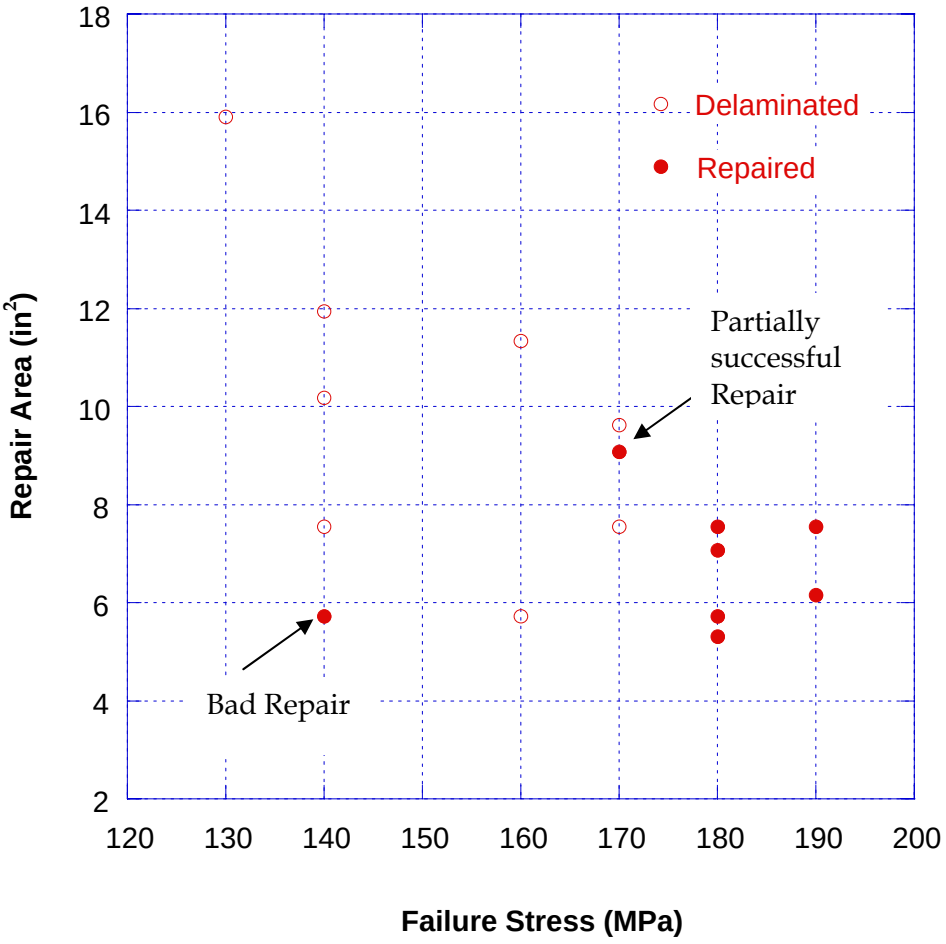

Figure 11 Failure stress measured for compression-compression fatigue loading of delaminated and repaired composite laminates

4.4 Discussion

Discussions with Mr Claude Lelievre at QETE (Quality Engineering Test Establishment), Canada, revealed that the original manufacture of the laminates by Bombardier was problematic with a second set of panels needing to be made. Despite the second set of panels being C-scanned and shown to have good quality (Figure 12), unexpected delamination growth was observed for some panels during injection repair (Figure 13). These delamination growths could not be traced to any errors in the injection process. Possible explanations offered by Mr Lelievre were that defects existed near the delaminations or that the delamination process using the stainless steel ball had caused delamination in a weakened area adjacent to the countersunk hole.

Mr Lelievre suggested that the manufacturing quality may have been variable with voided or weak areas existing in some areas of the second batch of panels. C-scan analysis of the panels that were injection repaired would have identified any delamination growth and

would have been discarded. As such, the repaired panels would have been filtered and had poorer quality laminates removed from the fatigue testing set.

Further work may be needed to determine if the poorer results obtained for the baseline and damaged coupons tended to come from one panel or from specific areas of original panels. An examination of the location of the specimens taken from the three original panels is provided in Appendix D. Panel 1 exhibited a good distribution of performance for the baseline, damaged and repaired panels. Repaired panels that surrounded a region where a failed resin injection had occurred showed a range of fatigue performance not indicating any correlation with a potentially poor region and lower fatigue resistance. Panel 2 also showed a good distribution in fatigue results for the three types of specimens with the low result for the repaired specimen 2.19 due to some problems in the injection repair. Panel 3 showed, on average, better fatigue performance for the baseline and damaged panels with no repaired coupons being taken from this panel. In summary, there appears to be little correlation in the results and the location from which panels were taken. The relatively small numbers of each coupon type taken from each of the panels makes any trends difficult to establish, however, if results from the other specimens that were tested by the Canadian Forces and the Swiss Air Force are considered, then clearer trends may be identified.

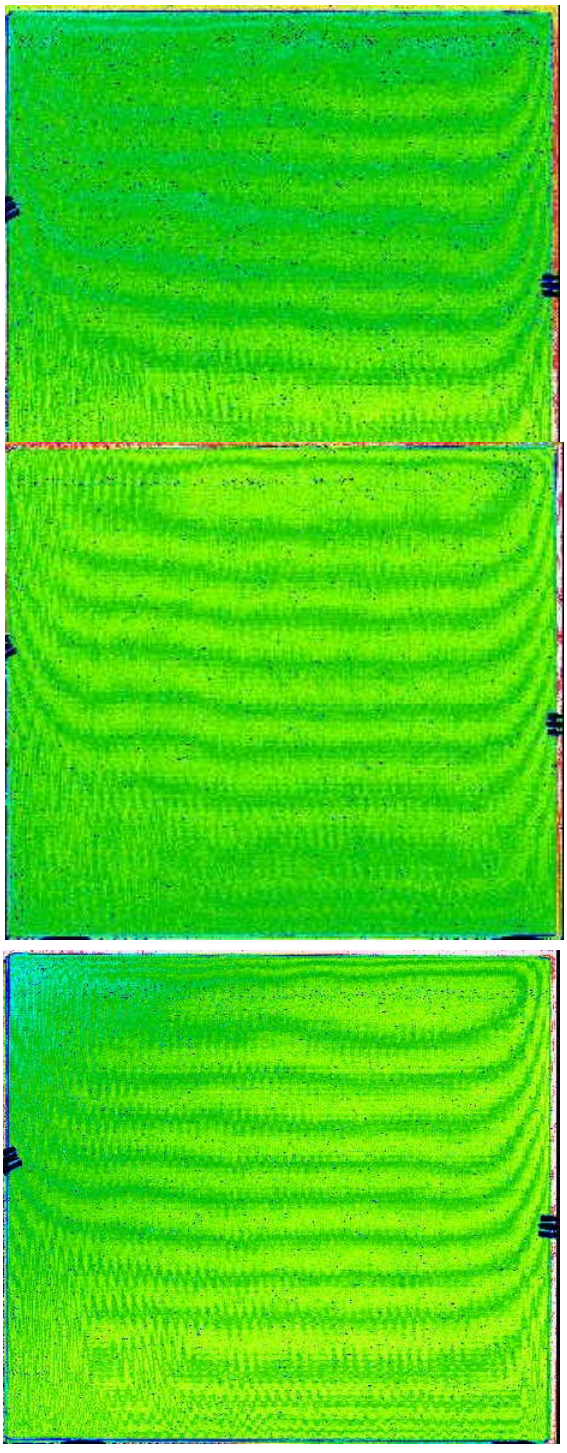

Figure 12 C-scan results for the three panels manufactured for preparation of the resin injection repair fatigue studies

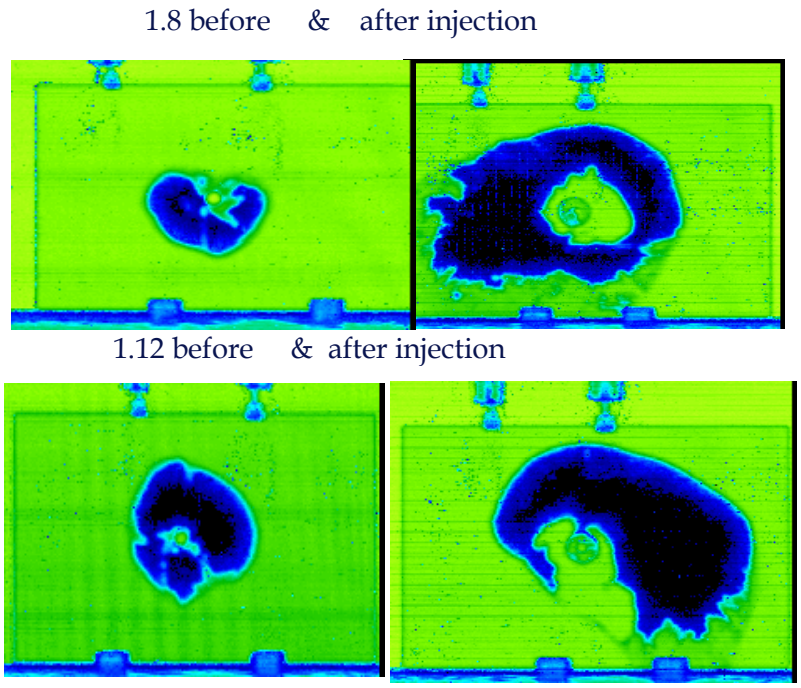

Figure 13 Examples of damaged panels C-scanned before and after resin injection, showing the increase in the delamination area caused by the resin injection process

4.5 Conclusions

There is a clear difference in the compression-compression fatigue strength of composite laminates that are damaged and repaired with resin injection. Resin injection repaired laminates exhibit similar average performance to baseline laminates and a higher failure stress than damaged laminates. The repaired laminates showed a more uniform distribution in failure stresses than either baseline or damaged laminates. The reduction in spread of the failure stresses for the repaired laminates may have been related to a reduced range of delamination areas compared with the damaged laminates, although delamination area and failure stress were only weakly correlated. Cross-section examination of the damaged and repaired composite samples should be undertaken to verify the effectiveness of the resin injection process, although the fatigue results suggest some measurable benefit.

5. References

1 K. Y. Blohowiak, J. H. Osborne, K. A. Krienke, D. F. Sekits, " *Sol-gel surface treatments for adhesive bonding of titanium and aluminium structures*", SAMPE Technical Conference, 28, pp. 440-446, SAMPE, Covina, CA, USA, 1996.

2 D. B. McCray and J. J. Mazza, "*Optimization of Sol-Gel Surface Preparations for Repair Bonding of Aluminum Alloys*", SAMPE 2000, Long Beach, CA, May 2000

3 Australian Air Publication 7021.016-2, "*Composite and Adhesive Bonded Repairs, Repair Fabrication and Application Procedures*", Royal Australian Air Force, 9 April, 2003

4 ASTM, Annual Book of Standards, Section 15, vol. 15.06, Adhesives. Philadelphia: ASTM, 1995-ASTM D3762, *Adhesive bonded surface durability of aluminium*

5 A. N. Rider, "*The Durability of Epoxy Adhesive Bonds formed with Titanium Alloy*", DSTO-TR-1333, DSTO, Melbourne, Australia, August, 2002.

6 A. N. Rider, " *Surface Preparation of 17-7 PH Sstainless Steel for Adhesive Bonding using FM300*", DSTO-CR-0263, DSTO, Melbourne, September, 2005.

7 Eric Pomerleau and Martin Vallerand, "*CREDP Task T-Test Plan for Resin Injection Technique Evaluation*", SES-3406, Bombardier Inc., June 1998.

8 Suppliers Advanced Composite Materials Association, "*Compression After Impact Properties of Oriented Fiber-Resin Composites*", SACMA SRM 2-88.

Appendix A: Surface Pretreatment Procedures

A.1. DSTO/RAAF Grit-blast and Silane Treatment

The DSTO/RAAF surface preparation procedure included the following steps:

1. The plates were wiped with tissue using analytical grade methyl ethyl ketone (MEK) to remove gross contamination.
2. Scotchbrite 3M No. 447 pad was used to abrade the adherend surface with MEK. The surface was first abraded in one direction for two minutes, then abraded in a direction 90° to the original direction until all original scratches were removed. The area was kept wet with MEK while abrading.
3. The adherend was wiped with MEK and tissues in the most recent direction (along the plate) to remove debris from the previous operation. This was continued until the tissues came up clean. Particular attention was given to the plate mid-span.
4. Distilled water and tissues were used to wipe the adherend surface again (along the plate).
5. Step 2 was repeated using distilled water in place of MEK.
6. Step 3 was repeated using distilled water in place of MEK.
7. The water break test was applied for 15 seconds to ensure a contaminant-free surface. The adherend was held at 45° and a squeeze bottle was used to apply distilled water.
8. The adherend was dried in an air-circulating oven for 20 minutes at 80°C.
9. The adherend was cooled to 35°C or less.
10. The bonding surface was grit blasted with 50 μm aluminium oxide grit using dry nitrogen gas as a propellant, with a pressure of approximately 450 kPa.
11. The adherend was submerged in a one percent aqueous solution of γ-glycidoxypropyl trimethoxy silane (γ-GPS) for 10 minutes. This solution consisted of 1% γ-GPS + 99% deionised or distilled water.
12. The adherend was dried in an air-circulating oven for one hour at 110°C.
13. The adherend was cooled to below 35°C.
14. If a primer step was used, BR-127 primer was applied using an airbrush with 30 psi nitrogen pressure and a working distance of 15 to 20 cm. The coating was considered thick enough when a uniform translucent straw colour could be observed on the grit-blasted and silane-treated surface. Previous testing with a Fischer Permascope E110, utilising a T3.3 eddy current probe, on polished aluminium surfaces indicated that the primer thickness corresponding to this colour was between 1.5-2□m.
15. The surfaces were bonded within one hour of being prepared to prevent contamination.

A.2. Task AF Boeing Wedge Test Data

Al7075-T76 unclad
Solvent degrease, water break, grit blast, silane
Bond FM300-2K

time (h)	sqrt time (h)	crack1	crack 2	crack 3	crack 4	crack 5	Crack average (m)	SD	95% CL	G_I(J/m^2)	crack(mm)
0	0	39.6	39.55	36.5	37.4	40.4	0.03869	1.65469	1.450373	1.51E+03	38.69
23.3	4.827007	41.95	39.75	36.6	37.4	40.4	0.03922	2.196759	1.925509	1.43E+03	39.22
47.3	6.8775	42.25	40.2	37.25	37.7	40.7	0.03962	2.104935	1.845023	1.38E+03	39.62
71	8.42615	42.45	40.2	37.45	37.85	40.7	0.03973	2.079243	1.822503	1.37E+03	39.73
94.3	9.710819	42.45	40.2	37.85	38.05	40.85	0.03988	1.944094	1.704042	1.35E+03	39.88
166	12.8841	42.6	40.3	38.05	38.35	41.25	0.04011	1.928536	1.690405	1.32E+03	40.11
190	13.78405	42.7	40.6	38.25	38.65	41.3	0.0403	1.855734	1.626593	1.29E+03	40.3
214.3	14.63899	42.8	41	38.8	38.65	41.3	0.04051	1.767201	1.548992	1.27E+03	40.51
238.8	15.45316	42.8	41.2	39.15	38.8	41.35	0.04066	1.664857	1.459285	1.25E+03	40.66
Cohesive Failure (%)		94	94	98	100	100	97.2				
Wedge thickness(mm)							0.003088				

Al7075-T76 unclad
Solvent degrease, water break, grit blast, silane, BR127 prime
Bond FM300-2K

time (h)	sqrt time (h)	crack1	crack 2	crack 3	crack 4	crack 5	Crack average(m)	SD	95% CL	G_I(J/m^2)	crack(mm)
0	0	36.5	37	35	37.05	36.95	0.0365	0.866747	0.871621	1.88E+03	36.5
23.3	4.827007	36.6	37.5	35.5	37.05	37.35	0.0368	0.803897	0.839425	1.83E+03	36.8
47.3	6.8775	37.7	38.25	35.75	37.6	37.95	0.03745	0.98298	0.928226	1.71E+03	37.45
71.3	8.443933	38.45	39.1	36.85	38.8	38.1	0.03826	0.872783	0.874651	1.58E+03	38.26
94	9.69536	38.55	39.25	37.2	38.8	38.2	0.0384	0.772172	0.822695	1.55E+03	38.4
118	10.86278	38.6	39.35	37.45	38.8	38.45	0.03853	0.693361	0.779581	1.53E+03	38.53
141.3	11.88697	38.6	39.35	37.65	38.8	38.6	0.0386	0.613392	0.733248	1.52E+03	38.6
165.3	12.8569	38.6	39.35	37.65	38.8	38.6	0.0386	0.613392	0.733248	1.52E+03	38.6
236.3	15.37205	38.95	40.3	38.2	39.85	39.25	0.03931	0.811942	0.843615	1.42E+03	39.31
Cohesive Failure(%)		100	85	90	90	95	92				
Wedge Thickness (m)		3.09	3.09	3.11	3.07	3.08	0.003088				

Al7075-T6 clad
Solvent degrease, water break, grit blast, silane, BR127 prime
Bond FM300-2K

time (h)	sqrt time (h)	crack1	crack 2	crack 3	crack 4	crack 5	Crack average (m)	SD	95% CL	G_I(J/m^2)	crack(mm)
0	0	39.7	37.25	39.6	39.4	41	0.03939	1.352036	1.18509	1.41E+03	39.39
26	5.09902	43.55	41.2	40.95	41.3	43.05	0.04201	1.197602	1.049725	1.33E+03	42.01
41.3	6.426508	44.25	42.1	41.05	41.5	44.25	0.04263	1.525041	1.336733	1.25E+03	42.63
71	8.42615	45.4	44.4	41.05	44.6	47.7	0.04463	2.39207	2.096703	1.04E+03	44.63
95	9.746794	46.3	45.65	41.85	47.2	48.85	0.04597	2.597739	2.276977	9.28E+02	45.97
166	12.8841	46.55	46.5	42.45	48	49.1	0.04652	2.520565	2.209332	8.85E+02	46.52
190	13.78405	47.05	46.5	43.8	48	49.4	0.04695	2.076054	1.819708	8.53E+02	46.95
214	14.62874	47.3	46.8	44.7	48.25	49.6	0.04733	1.816453	1.592162	8.26E+02	47.33
237.3	15.40454	47.65	46.8	44.7	48.25	49.6	0.0474	1.821744	1.596799	8.21E+02	47.4
Cohesive Failure (%)		30	40	50	35	20	35				
Wedge Thickness (m)							0.003088				

A.3. Boeing Wedge Test Failure Images

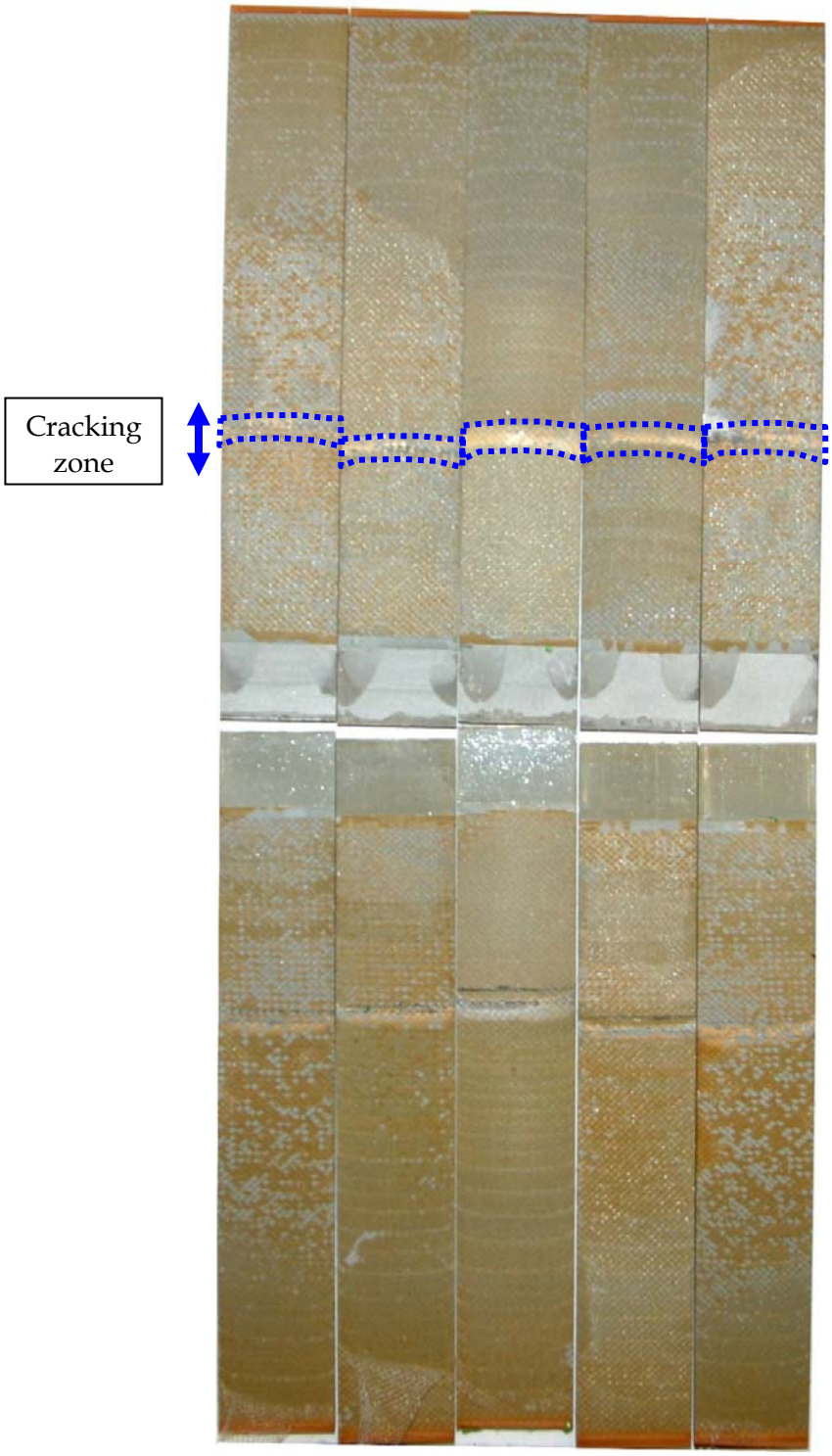

Al7075-T76 unclad aluminium treated with the grit blast and silane and bonded with FM300-2K.

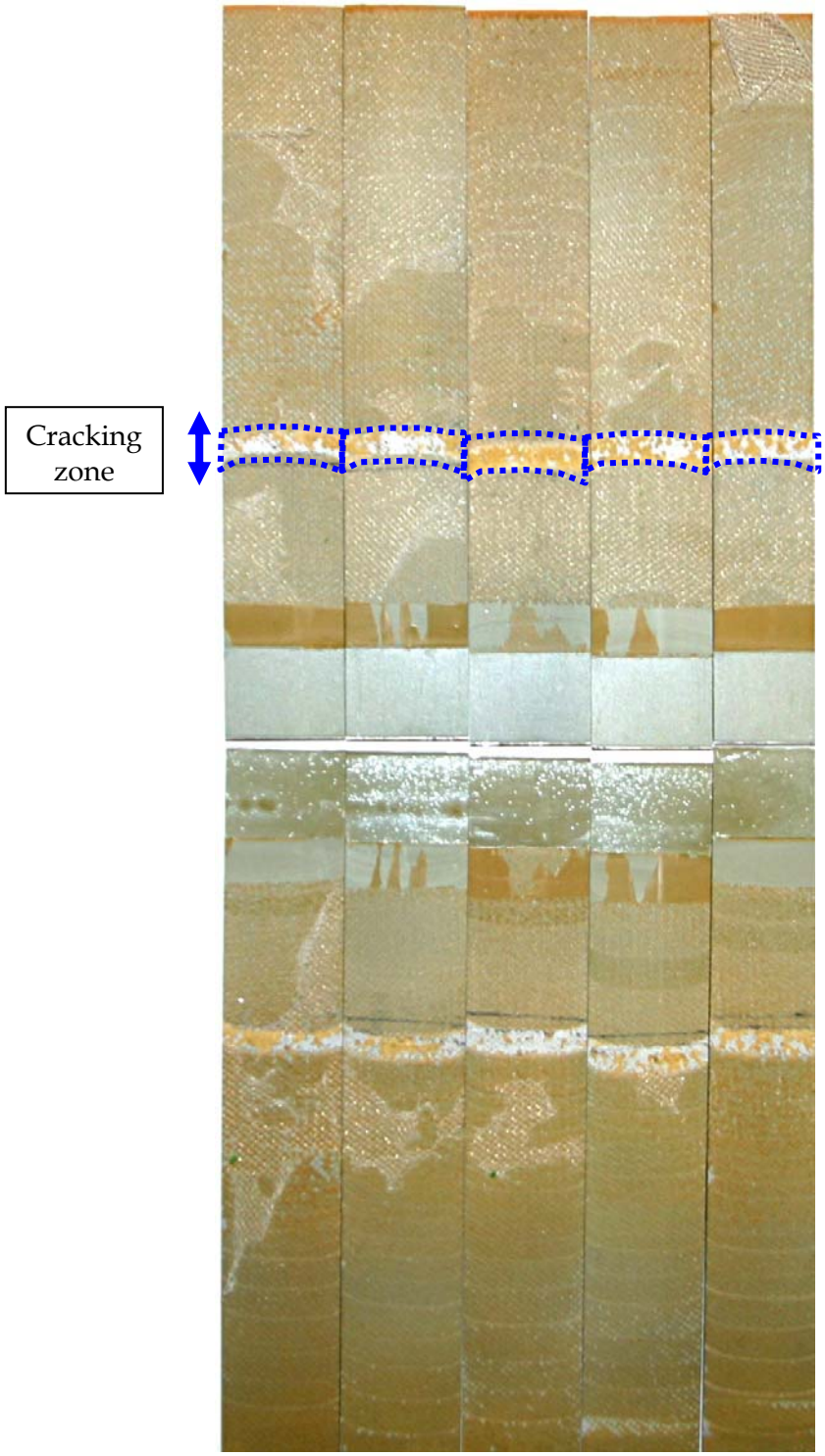

Al7075-T76 unclad aluminium treated with the grit blast and silane, primed with BR-127 and bonded with FM300-2K.

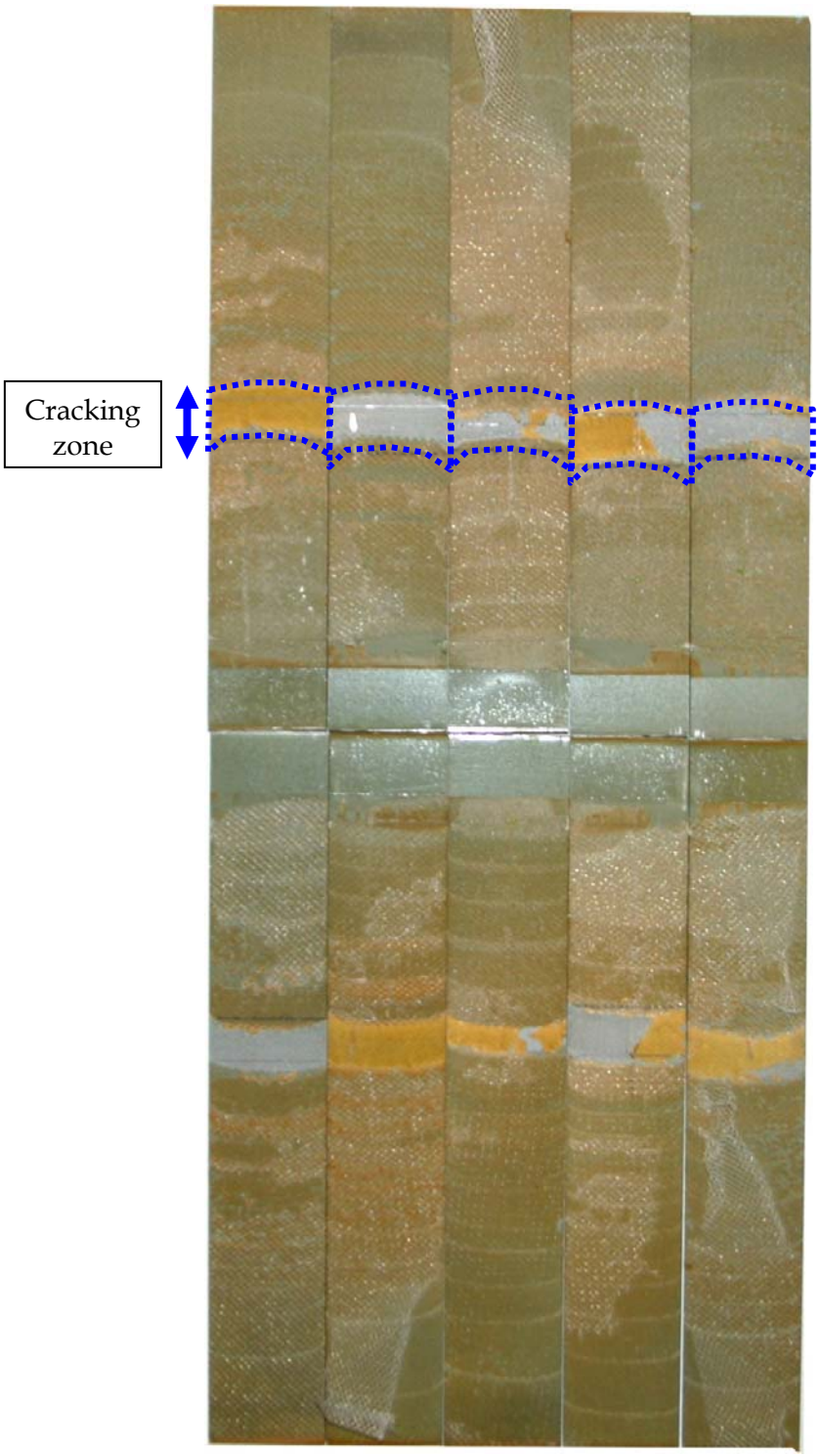

Al7075-T6 clad aluminium treated with the grit blast and silane, primed with BR-127 and bonded with FM300-2K.

Appendix B:

B.1. Sol-gel treatment

The recently developed AC-130® treatment developed and licensed by Boeing and sold by AC Tech used similar steps to those listed in Appendix A.1, but replaced the epoxy silane with the AC-130® solution detailed below.

Table B1 Chemicals used in the AC-130® solution

Material	Volume (mL)
Glacial Acetic Acid	0.4
Zirconium (IV) Propoxide (70wt%)	1.0
γ-glycidoxypropyltrimethoxysilane (γ-GPS)	1.9
Distilled Water	96.7

B.2. Task AF Boeing Wedge Test Data

Ti-6A1-4V
Sol/Degrease,W/Break Test,G/Blast,Sol-Gel
FM300-2K
Sol-Gel
Depot

time (h)	sqrt time (h)	crack1	crack 2	crack 3	crack 4	crack 5	Crack average(m)	SD	95% CL	G_I(J/m2)	crack(mm)
0	0	41.6	36.5	40.7	39.55	38.45	0.03936	1.991042	1.745194	9.88E+02	39.36
25.3	5.029911	55.2	48.5	51	49.65	49.2	0.05071	2.670768	2.340988	3.74E+02	50.71
49.3	7.021396	57.15	49.95	54.9	51.55	51.25	0.05296	2.970354	2.603582	3.17E+02	52.96
71	8.42615	60.5	50.95	57.75	53.15	54.95	0.05546	3.76105	3.296645	2.65E+02	55.46
95	9.746794	61.65	51.35	57.75	53.65	55.6	0.056	3.946201	3.458934	2.55E+02	56
119	10.90871	61.95	52.1	58.3	54.35	55.9	0.05652	3.784277	3.317004	2.46E+02	56.52
142.3	11.92896	61.95	52.35	58.3	54.35	55.9	0.05657	3.712243	3.253865	2.45E+02	56.57
166.3	12.89574	62	52.45	58.3	54.35	56	0.05662	3.697736	3.241149	2.44E+02	56.62
237.3	15.40454	63.1	56.15	60.3	56.8	57.85	0.05884	2.857315	2.504501	2.11E+02	58.84
Cohesive(%)		5	45	25	20	1	19.2				
Wedge Thickness (mm)		2.22	2.22	2.23	2.23	2.24	2.23				

Ti-6A1-4V
Sol/Degrease W/Break Test,G/Blast,Silane,BR127 Prime
FM300-2K

time (h)	sqrt time (h)	crack1	crack 2	crack 3	crack 4	crack 5	Crack average (mm)	SD	95% CL	G_I(J/m^2)	crack(mm)
0	0	39.2	38.65	38.1	39.65	38.6	0.03884	0.597286	0.523534	1.03E+03	38.84
25	5	46.65	47.35	48.25	47.75	46.2	0.04724	0.824924	0.723065	4.88E+02	47.24
49	7	49.65	49.25	51.45	49.95	49.4	0.04994	0.884873	0.775611	3.94E+02	49.94
71	8.42615	53.2	53.85	57.05	54	52.35	0.05409	1.778131	1.558572	2.90E+02	54.09
95	9.746794	53.45	54.8	57.95	55.25	53.6	0.05501	1.814318	1.590291	2.71E+02	55.01
118.3	10.87658	54.5	55.65	58.1	55.5	54.65	0.05568	1.444213	1.265885	2.59E+02	55.68
142	11.91638	54.55	55.65	58.1	55.55	54.95	0.05576	1.383112	1.212329	2.58E+02	55.76
166	12.8841	54.85	55.75	58.2	55.55	54.95	0.05586	1.363085	1.194774	2.56E+02	55.86
237	15.3948	56.35	58.45	59.9	57.25	57.9	0.05797	1.332573	1.16803	2.22E+02	57.97
Cohesive(%)		30	5	3	35	20	18.6				
Wedge Thickness (mm)		2.22	2.22	2.22	2.22	2.22	2.22				

301 STAINLESS STEEL
Sol/Degrease, Grit Blast, AC-130
Bond FM300-2K

time (h)	sqrt time (h)	crack1	crack 2	crack 3	crack 4	crack 5	Crack average (m)	SD	95% CL	G_I(J/m^2)	crack(mm)
0	0	34.8	35.6	32.3	34.9	36.1	0.03474	1.463899	1.28314	9.60E+02	34.74
23	4.795832	37.05	37.7	34.5	36.65	37.9	0.03676	1.358952	1.191152	7.71E+02	36.76
47	6.855655	38.75	39.25	38	38.6	39.25	0.03877	0.520336	0.456087	6.26E+02	38.77
72	8.485281	39.25	40.1	38.95	39.75	40.45	0.0397	0.610328	0.534966	5.71E+02	39.7
95	9.746794	39.85	40.65	39.75	40.45	41.3	0.0404	0.632456	0.554362	5.33E+02	40.4
165.3	12.8569	40.85	41.5	41.25	42.1	42.05	0.04155	0.532682	0.466908	4.78E+02	41.55
189	13.74773	41.6	41.85	41.4	42.5	42.35	0.04194	0.47355	0.415078	4.61E+02	41.94
213.3	14.60479	41.8	42.05	41.65	42.7	42.4	0.04212	0.430987	0.37777	4.53E+02	42.12
237	15.3948	42.25	42.2	41.75	42.8	42.55	0.04231	0.395917	0.34703	4.45E+02	42.31
Cohesive failure (%)		50	50	35	10	50	39				
Wedge Thickness (mm)		3.08	3.09	3.11	3.11	3.11	3.10				

PH13-8MO
Solvent Degrease,G/Blast,Sol Gel
Bond FM300-2K
Sol-Gel
Depot

time (h)	sqrt time (h)	crack1	crack 2	crack 3	crack 4	crack 5	Crack average (m)	SD	95% CL	G_I(J/m^2)	crack(mm)
0	0	**49.95**	41.25	43.45	41.9	39.05	0.041413	1.825457	1.788915	1.08E+03	41.4125
24.3	4.929503	**50.9**	48.75	51.45	49.6	47.1	0.049225	1.810387	1.774146	5.60E+02	49.225
48	6.928203	**51.4**	52	56.25	51.65	50.7	0.05265	2.462045	2.41276	4.32E+02	52.65
71.3	8.443933	**52.85**	54.1	58.85	53	53.3	0.054813	2.731414	2.676737	3.70E+02	54.8125
142.3	11.92896	**54.4**	57	62.25	56	57.75	0.05825	2.76134	2.706064	2.93E+02	58.25
166.3	12.89574	**58.3**	57	62.95	56	58.8	0.058688	3.068761	3.00733	2.85E+02	58.6875
190	13.78405	**58.45**	57.85	63.15	56.1	58.95	0.059013	2.997603	2.937597	2.79E+02	59.0125
214	14.62874	**58.85**	57.85	64.15	56.45	59.65	0.059525	3.35	3.28294	2.70E+02	59.525
237.3	15.40454	**59.3**	58.55	65.05	56.5	60.85	0.060238	3.667509	3.594093	2.57E+02	60.2375
Cohesive Failure (%)		**35**	35	40	20	40	33.7	8.196829	8.032744		
Wedge Thickness (mm)		**2.2** Thicker wedge used	1.54	1.55	1.54	1.56	1.55				

B.3. Boeing Wedge Test Failure Images

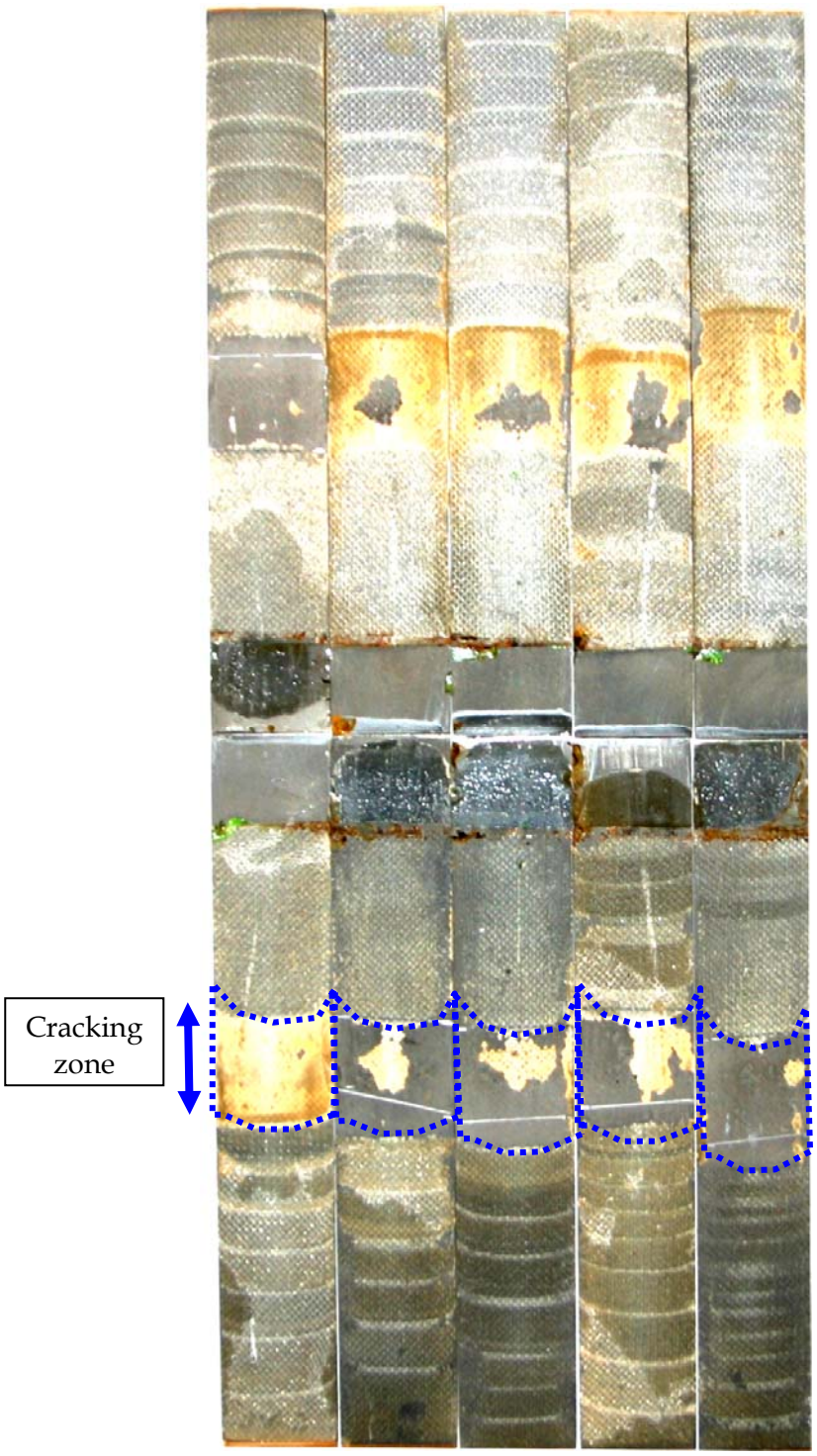

Ti 6Al-4V treated with the grit blast and sol-gel method and bonded with FM300-2K.

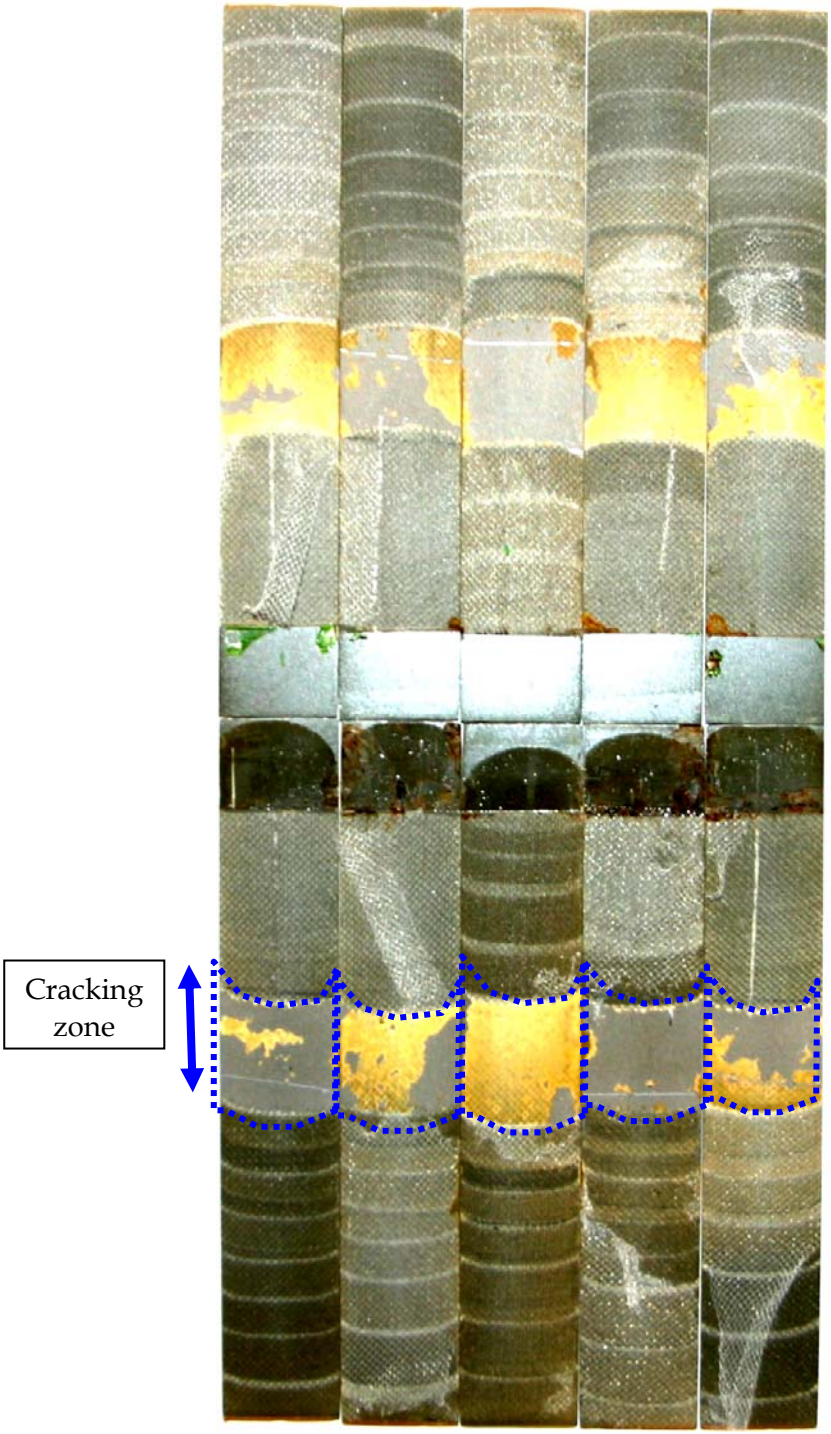

Ti 6Al-4V treated with the grit blast and silane, primed with BR-127 and bonded with FM300-2K.

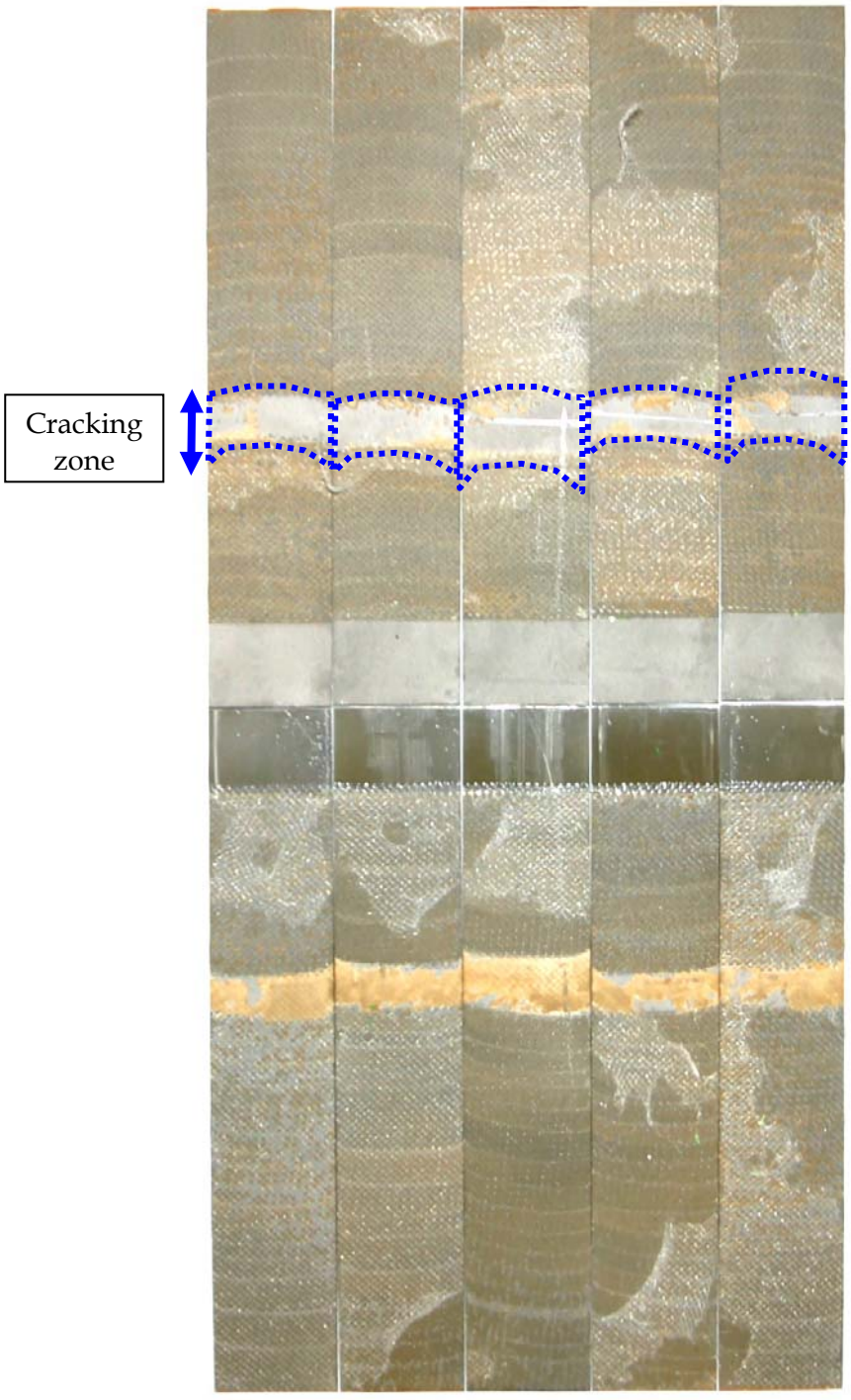

301 stainless steel treated with the grit blast and sol-gel and bonded with FM300-2K.

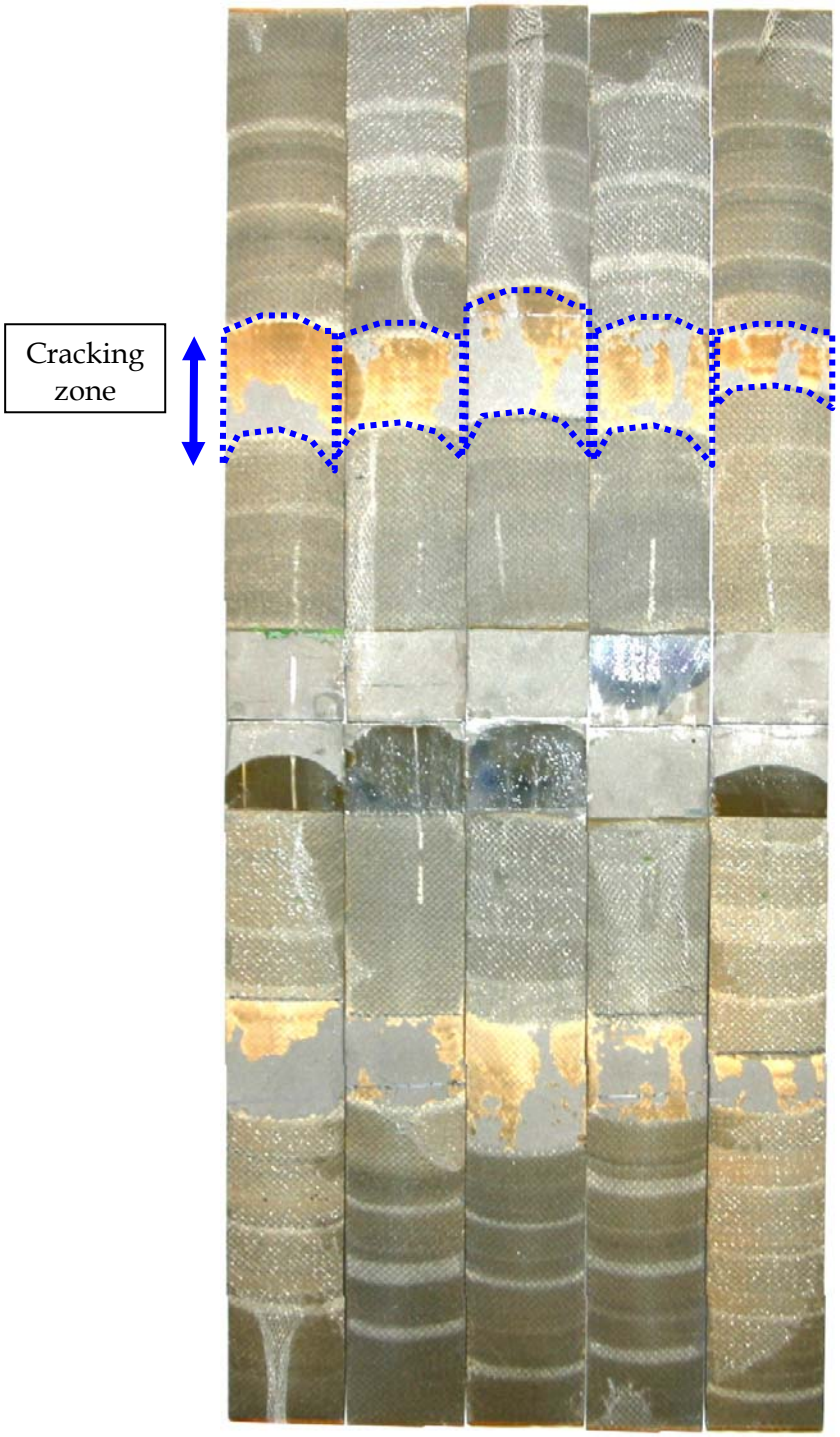

PH13-8Mo stainless steel treated with the grit blast and sol-gel and bonded with FM300-2K.

Appendix C: Compression-Compression Fatigue of Resin Injection Repairs-Task AI

	Task No	AIR04/241	Test No	FFL06/36	Lab Book	08/03
	Test Plan	FFLTP716	WA No	DSA21526	Pages	1165 to 1172 and 1174 to 1194

Test Title **CREDP Task AI - Fatigue testing of resin injection repaired composite laminates**

Customer` Andrew Rider PH Ext 7393

Objective **To evaluate the effectiveness of resin injection repairs in restoring the compression compression fatigue life of composite laminates with a delamination around a counter sunk hole.**

Test setup:

250 kN Instron running under MTS Basic Test Ware

Test Profile Name:

CREDP Task AI.tst

	Thickness mm												
Specimen	**1**	**2**	**3**	**4**	**Width mm**	**Area mm^2**	**frequency**	**Stress Mpa**	**Force kN**	**Set Point kN**	**Amplitude kN**	**Cycles**	**Comments**
1.15	5.034	5.035	4.983	4.971	178.56	893.827	5Hz	120	107.259	-58.993	48.267	514,770	Specimen removed without failure
2.6	4.987	4.989	5.012	5.012	177.74	888.700	5Hz	140	124.418	-68.430	55.988	420,003	Specimen removed without failure

Specimen	1	2	3	4	Width mm	Area mm^2	frequency	Stress Mpa	Force kN	Set Point kN	Amplitude kN	Cycles	Comments
3.7	5.042	5.02	4.989	4.958	179.1	895.903	5Hz	160	143.344	-78.839	64.505	527,550	Increase load to 180 Mpa
						895.903	5Hz	180	161.263	-88.694	72.568	838,004	Increase load to 200 Mpa
						895.903	5Hz	200	179.181	-98.549	80.631	858,610	Failure occurred at 858,610 cycles total
3.18	4.982	4.887	4.756	4.384	178.34	847.516	5Hz	200	169.503	-93.227	76.276	737	Failed
3.13	4.952	4.909	4.943	4.956	177.47	876.702	5Hz	190	166.573	-91.615	74.958	1867	
1.14	4.935	4.991	5.003	5.061	177.67	887.906	5Hz	180	159.823	-87.903	71.920		M/C stopped at 793,011 cycles with a displacement limit tripped. When I attempted to restart M/C, specimen failed instantly because of displacement error.
2.6	5.005	4.994	5.012	5.029	177.74	890.477	5Hz	160	142.476	-78.362	64.114	100,000	set to 170 Mpa
						890.477	5Hz	170	151.381	-83.260	68.122	200,000	increase stress by 10 Mpa

Specimen	1	2	3	4	Width mm	Area mm^2	frequency	Stress Mpa	Force kN	Set Point kN	Amplitude kN	Cycles	Comments
						890.477	5Hz	180	160.286	-88.157	72.129	300,000	increase stress by 10 Mpa
						890.477	5Hz	190	169.191	-93.055	76.136	400,000	increase stress by 10 Mpa
						890.477	5Hz	200	178.095	-97.953	80.143	407,852	Specimen failed after 7852 cycles at 200 Mpa
	1.15	5.051	5.027	4.987	4.994	178.48	895.033	5Hz	160	143.205	-78.763	64.442	100,000	increase stress by 10 Mpa
							895.033	5Hz	170	152.156	-83.686	68.470	151,018	Specimen failed after 51,018 cycles at 170 Mpa
	3.17	4.444	4.794	4.861	4.938	179.52	854.381	5Hz	160	136.701	-75.185	61.515	181	Specimen failed after 181 cycles at 160 Mpa
	1.16	5.015	4.947	4.916		177.1	878.298	5Hz	120	105.396	-57.968	47.428	100,000	increase stress by 10 Mpa
							878.298	5Hz	130	114.179	-62.798	51.380	200,000	increase stress by 10 Mpa
							878.298	5Hz	140	122.962	-67.629	55.333	248,281	Specimen failed after 48,281 cycles at 140 Mpa

Specimen	1	2	3	4	Width mm	Area mm^2	frequency	Stress Mpa	Force kN	Set Point kN	Amplitude kN	Cycles	Comments
2.16	4.65	4.65	4.631	4.704	178.34	830.841	5Hz	120	99.701	-54.836	44.865	100,000	increase stress by 10 Mpa
						830.841	5Hz	130	108.009	-59.405	48.604	200,000	increase stress by 10 Mpa
						830.841	5Hz	140	116.318	-63.975	52.343	300,000	increase stress by 10 Mpa
						830.841	5Hz	150	124.626	-68.544	56.082	400,000	increase stress by 10 Mpa
						830.841	5Hz	160	132.935	-73.114	59.821	500,000	increase stress by 10 Mpa
						830.841	5Hz	170	141.243	-77.684	63.559	500,532	Specimen failed after 532 cycles at 170 Mpa
3.15	4.945	4.936	4.966		178.38	882.803	5Hz	120	105.936	-58.265	47.671	100,000	increase stress by 10 Mpa
						882.803	5Hz	130	114.764	-63.120	51.644	200,000	increase stress by 10 Mpa
						882.803	5Hz	140	123.592	-67.976	55.617	260,508	Specimen failed after 60,508 cycles at 140 Mpa

Specimen	1	2	3	4	Width mm	Area mm^2	frequency	Stress Mpa	Force kN	Set Point kN	Amplitude kN	Cycles	Comments
2.8	4.933	4.959	4.965		178.08	881.912	5Hz	120	105.829	-58.206	47.623	100,000	increase stress by 10 Mpa
						881.912	5Hz	130	114.648	-63.057	51.592	200,000	increase stress by 10 Mpa
						881.912	5Hz	140	123.468	-67.907	55.560	202,934	Specimen failed after 2,934 cycles at 140 Mpa
3.3	4.39	4.755	4.869		178.58	834.207	5Hz	120	100.105	-55.058	45.047	100,000	increase stress by 10 Mpa
						834.207	5Hz	130	108.447	-59.646	48.801	113,453	Specimen failed after 13,453 cycles at 130 Mpa
2.7	4.969	5	4.998		178.34	889.738	5Hz	120	106.769	-58.723	48.046	100,000	increase stress by 10 Mpa
						889.738	5Hz	130	115.666	-63.616	52.050	200,000	increase stress by 10 Mpa
						889.738	5Hz	140	124.563	-68.510	56.054	300,000	increase stress by 10 Mpa
						889.738	5Hz	150	133.461	-73.403	60.057	400,000	increase stress by 10 Mpa

Specimen	1	2	3	4	Width mm	Area mm^2	frequency	Stress Mpa	Force kN	Set Point kN	Amplitude kN	Cycles	Comments
						889.738	5Hz	160	142.358	-78.297	64.061	500,000	increase stress by 10 Mpa
						889.738	5Hz	170	151.256	-83.191	68.065	500,215	Specimen failed after 215 cycles at 170 Mpa
1.18	4.891	4.868	4.664		178.14	856.438	5Hz	120	102.773	-56.525	46.248	100,000	increase stress by 10 Mpa
						856.438	5Hz	130	111.337	-61.235	50.102	200,000	increase stress by 10 Mpa
						856.438	5Hz	140	119.901	-65.946	53.956	300,000	increase stress by 10 Mpa
						856.438	5Hz	150	128.466	-70.656	57.810	400,000	increase stress by 10 Mpa
						856.438	5Hz	160	137.030	-75.367	61.664	474,659	Specimen failed after 74,659 cycles at 160 Mpa
3.10	5.05	5.072	5.036		178.22	900.486	5Hz	120	108.058	-59.432	48.626	100,000	increase stress by 10 Mpa
						900.486	5Hz	130	117.063	-64.385	52.678	200,000	increase stress by 10 Mpa

Specimen	1	2	3	4	Width mm	Area mm^2	frequency	Stress Mpa	Force kN	Set Point kN	Amplitude kN	Cycles	Comments
						900.486	5Hz	140	126.068	-69.337	56.731	270,126	Specimen failed after 70,126 cycles at 140 Mpa
2.10	4.976	4.951	4.97		177.74	882.598	5Hz	160	141.216	-77.669	63.547	100,000	increase stress by 10 Mpa
						882.598	5Hz	170	150.042	-82.523	67.519	200,000	increase stress by 10 Mpa
						882.598	5Hz	180	158.868	-87.377	71.490	200,404	Specimen failed after 404 cycles at 180 Mpa
2.12	4.985	4.989	4.953		177.7	884.176	5Hz	160	141.468	-77.807	63.661	100,000	increase stress by 10 Mpa
						884.176	5Hz	170	150.310	-82.670	67.639	200,000	increase stress by 10 Mpa
						884.176	5Hz	180	159.152	-87.533	71.618	251,167	Specimen failed after 51,167 cycles at 180 Mpa
1.19	4.936	4.878	4.596		178.18	855.858	5Hz	160	136.937	-75.315	61.622	100,000	increase stress by 10 Mpa
						855.858	5Hz	170	145.496	-80.023	65.473	200,000	increase stress by 10 Mpa

Specimen	1	2	3	4	Width mm	Area mm^2	frequency	Stress Mpa	Force kN	Set Point kN	Amplitude kN	Cycles	Comments
						855.858	5Hz	180	154.054	-84.730	69.324	214,736	Specimen failed after 14,736 cycles at 180 Mpa
2.19	4.921	4.825	4.534		177.9	846.804	5Hz	120	101.616	-55.889	45.727	100,000	increase stress by 10 Mpa
						846.804	5Hz	130	110.085	-60.546	49.538	200,000	increase stress by 10 Mpa
						846.804	5Hz	140	118.553	-65.204	53.349	300,000	increase stress by 10 Mpa
						846.804	5Hz	150	127.021	-69.861	57.159	400,000	increase stress by 10 Mpa
						846.804	5Hz	160	135.489	-74.519	60.970	500,000	increase stress by 10 Mpa
						846.804	5Hz	170	143.957	-79.176	64.781	535,379	Specimen failed after 35,379 cycles at 170 Mpa
1.7	4.981	4.967	4.978		178.05	885.858	5Hz	120	106.303	-58.467	47.836	100,000	increase stress by 10 Mpa
						885.858	5Hz	130	115.162	-63.339	51.823	200,000	increase stress by 10 Mpa

Specimen	1	2	3	4	Width mm	Area mm^2	frequency	Stress Mpa	Force kN	Set Point kN	Amplitude kN	Cycles	Comments
						885.858	5Hz	140	124.020	-68.211	55.809	300,000	increase stress by 10 Mpa
						885.858	5Hz	150	132.879	-73.083	59.795	400,000	increase stress by 10 Mpa
						885.858	5Hz	160	141.737	-77.956	63.782	500,000	increase stress by 10 Mpa
						885.858	5Hz	170	150.596	-82.828	67.768	600,000	increase stress by 10 Mpa
						885.858	5Hz	180	159.454	-87.700	71.755	619,800	Specimen failed after 19,800 cycles at 180 Mpa
	1.6	4.985	5.017	4.996	178.26	891.181	5Hz	120	106.942	-58.818	48.124	100,000	increase stress by 10 Mpa
						891.181	5Hz	130	115.854	-63.719	52.134	200,000	increase stress by 10 Mpa
						891.181	5Hz	140	124.765	-68.621	56.144	300,000	increase stress by 10 Mpa
						891.181	5Hz	150	133.677	-73.522	60.155	400,000	increase stress by 10 Mpa
						891.181	5Hz	160	142.589	-78.424	64.165	500,000	increase stress by 10 Mpa

Specimen	1	2	3	4	Width mm	Area mm^2	frequency	Stress Mpa	Force kN	Set Point kN	Amplitude kN	Cycles	Comments
						891.181	5Hz	170	151.501	-83.325	68.175	600,000	increase stress by 10 Mpa
						891.181	5Hz	180	160.413	-88.227	72.186	612,190	Specimen failed after 12,190 cycles at 180 Mpa
	1.5	4.996	4.702	4.732	177.5	853.775	5Hz	120	102.453	-56.349	46.104	100,000	increase stress by 10 Mpa
						853.775	5Hz	130	110.991	-61.045	49.946	200,000	increase stress by 10 Mpa
						853.775	5Hz	140	119.529	-65.741	53.788	300,000	increase stress by 10 Mpa
						853.775	5Hz	150	128.066	-70.436	57.630	400,000	increase stress by 10 Mpa
						853.775	5Hz	160	136.604	-75.132	61.472	500,000	increase stress by 10 Mpa
						853.775	5Hz	170	145.142	-79.828	65.314	600,000	increase stress by 10 Mpa
						853.775	5Hz	180	153.680	-84.524	69.156	700,000	increase stress by 10 Mpa
						853.775	5Hz	190	162.217	-89.219	72.998	726,074	Specimen failed after 26,074 cycles at 190 Mpa

Specimen	1	2	3	4	Width mm	Area mm^2	frequency	Stress Mpa	Force kN	Set Point kN	Amplitude kN	Cycles	Comments
2.20	4.764	4.714	4.513		177.16	826.215	5Hz	120	99.146	-54.530	44.616	100,000	increase stress by 10 Mpa
						826.215	5Hz	130	107.408	-59.074	48.334	200,000	increase stress by 10 Mpa
						826.215	5Hz	140	115.670	-63.619	52.052	300,000	increase stress by 10 Mpa
						826.215	5Hz	150	123.932	-68.163	55.770	400,000	increase stress by 10 Mpa
						826.215	5Hz	160	132.194	-72.707	59.487	500,000	increase stress by 10 Mpa
						826.215	5Hz	170	140.457	-77.251	63.205	600,000	increase stress by 10 Mpa
						826.215	5Hz	180	148.719	-81.795	66.923	637,051	Specimen failed after 37,051 cycles at 180 Mpa
1.1	4.404	4.604	4.741		177.07	811.512	5Hz	120	97.381	-53.560	43.822	100,000	increase stress by 10 Mpa
						811.512	5Hz	130	105.497	-58.023	47.473	200,000	increase stress by 10 Mpa
						811.512	5Hz	140	113.612	-62.486	51.125	300,000	increase stress by 10 Mpa

Specimen	1	2	3	4	Width mm	Area mm^2	frequency	Stress Mpa	Force kN	Set Point kN	Amplitude kN	Cycles	Comments
1.1con't.						811.512	5Hz	150	121.727	-66.950	54.777	400,000	increase stress by 10 Mpa
						811.512	5Hz	160	129.842	-71.413	58.429	500,000	increase stress by 10 Mpa
						811.512	5Hz	170	137.957	-75.876	62.081	600,000	increase stress by 10 Mpa
						811.512	5Hz	180	146.072	-80.340	65.732	700,000	increase stress by 10 Mpa
						811.512	5Hz	190	154.187	-84.803	69.384	734,018	Specimen failed after 34,018 cycles at 190 Mpa
1.2	4.946	4.844	4.481		178.08	847.127	5Hz	120	101.655	-55.910	45.745	100,000	increase stress by 10 Mpa
						847.127	5Hz	130	110.126	-60.570	49.557	200,000	increase stress by 10 Mpa
						847.127	5Hz	140	118.598	-65.229	53.369	209,515	Specimen failed after 9,515 cycles at 140 Mpa Specimen appeared to be delaminated from commencement of test, suspect faulty repair.

Specimen	1	2	3	4	Width mm	Area mm^2	frequency	Stress Mpa	Force kN	Set Point kN	Amplitude kN	Cycles	Comments
1.3	4.981	4.844	4.444		178.14	847.293	5Hz	120	101.675	-55.921	45.754	100,000	increase stress by 10 Mpa
						847.293	5Hz	130	110.148	-60.581	49.567	200,000	increase stress by 10 Mpa
						847.293	5Hz	140	118.621	-65.242	53.379	300,000	increase stress by 10 Mpa
						847.293	5Hz	150	127.094	-69.902	57.192	400,000	increase stress by 10 Mpa
						847.293	5Hz	160	135.567	-74.562	61.005	500,000	increase stress by 10 Mpa
						847.293	5Hz	170	144.040	-79.222	64.818	600,000	increase stress by 10 Mpa
						847.293	5Hz	180	152.513	-83.882	68.631	613,614	Specimen failed after 13,614 cycles at 180 Mpa

Appendix D: Location of Specimens Taken from Original Panels

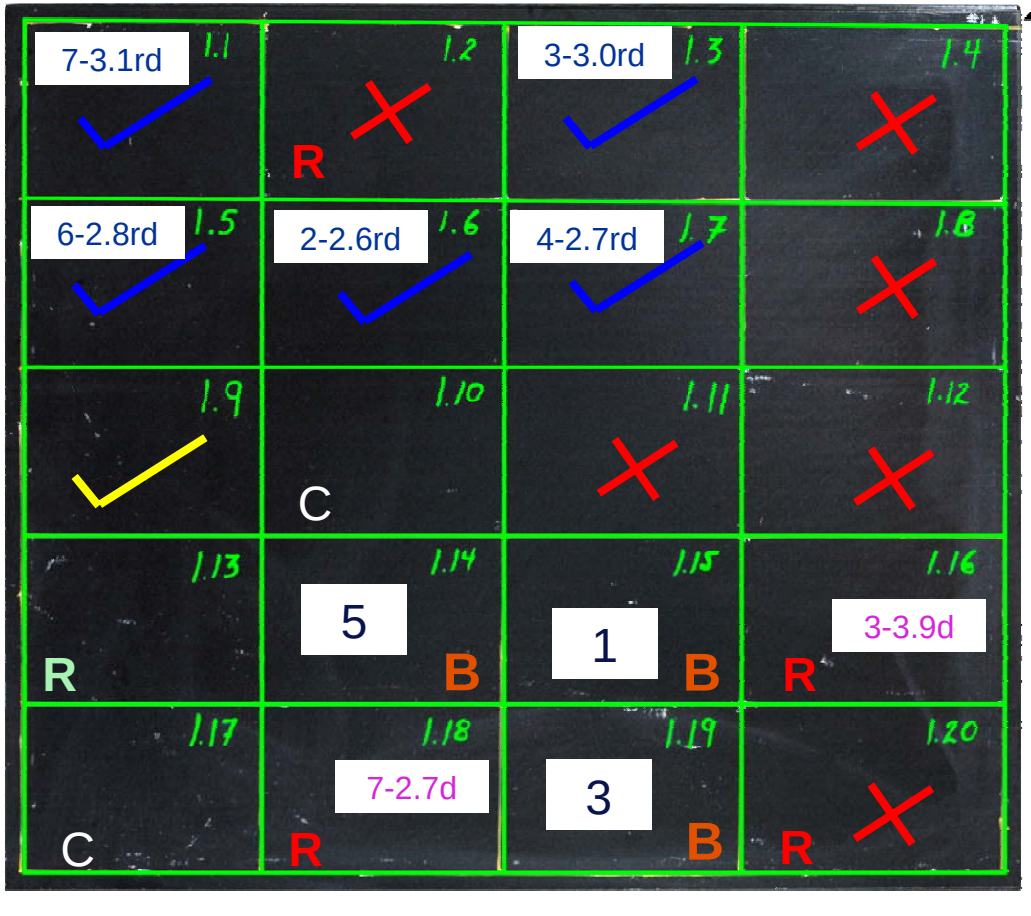

✓	Successful iniection
✗	Failed injection
✓	Partially Successful injection
S	Spare coupon
B	Baseline coupon
R	RAAF tested
R	RUAG injection test
CF	CF injection test

As manufactured Panel 1 with coupon locations identified. Numbers in white boxes represent baseline, bold black numeral, damaged, pink numeral with damage diameter and repaired test specimens, blue numeral with repaired damage diameter in inches. Numbers represent the fatigue resistance from worst (1) to best (7, 8 &9).

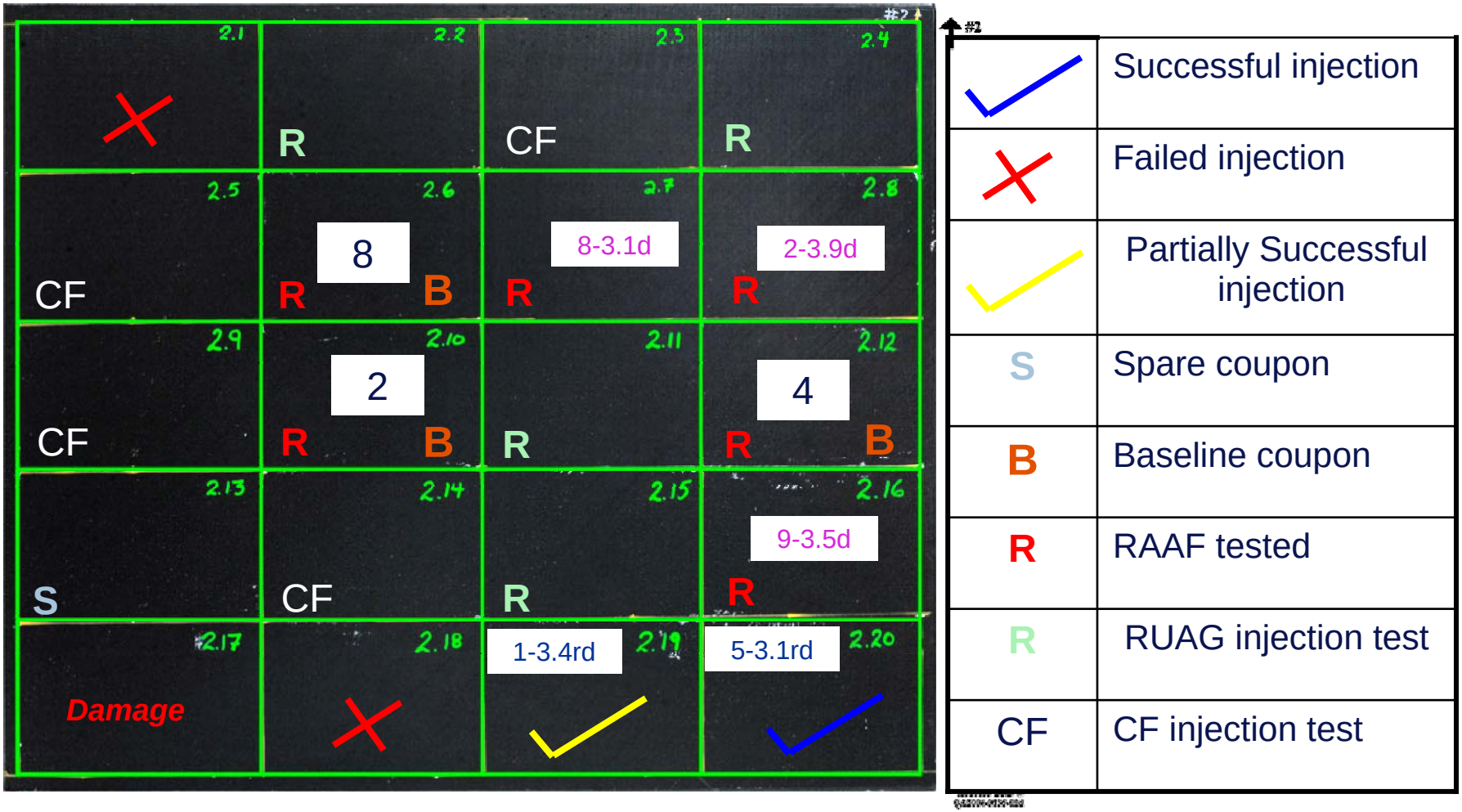

As manufactured Panel 2 with coupon locations identified. Numbers in white boxes represent baseline, bold black numeral, damaged, pink numeral with damage diameter and repaired test specimens, blue numeral with repaired damage diameter in inches. Numbers represent the fatigue resistance from worst (1) to best (7, 8 &9).

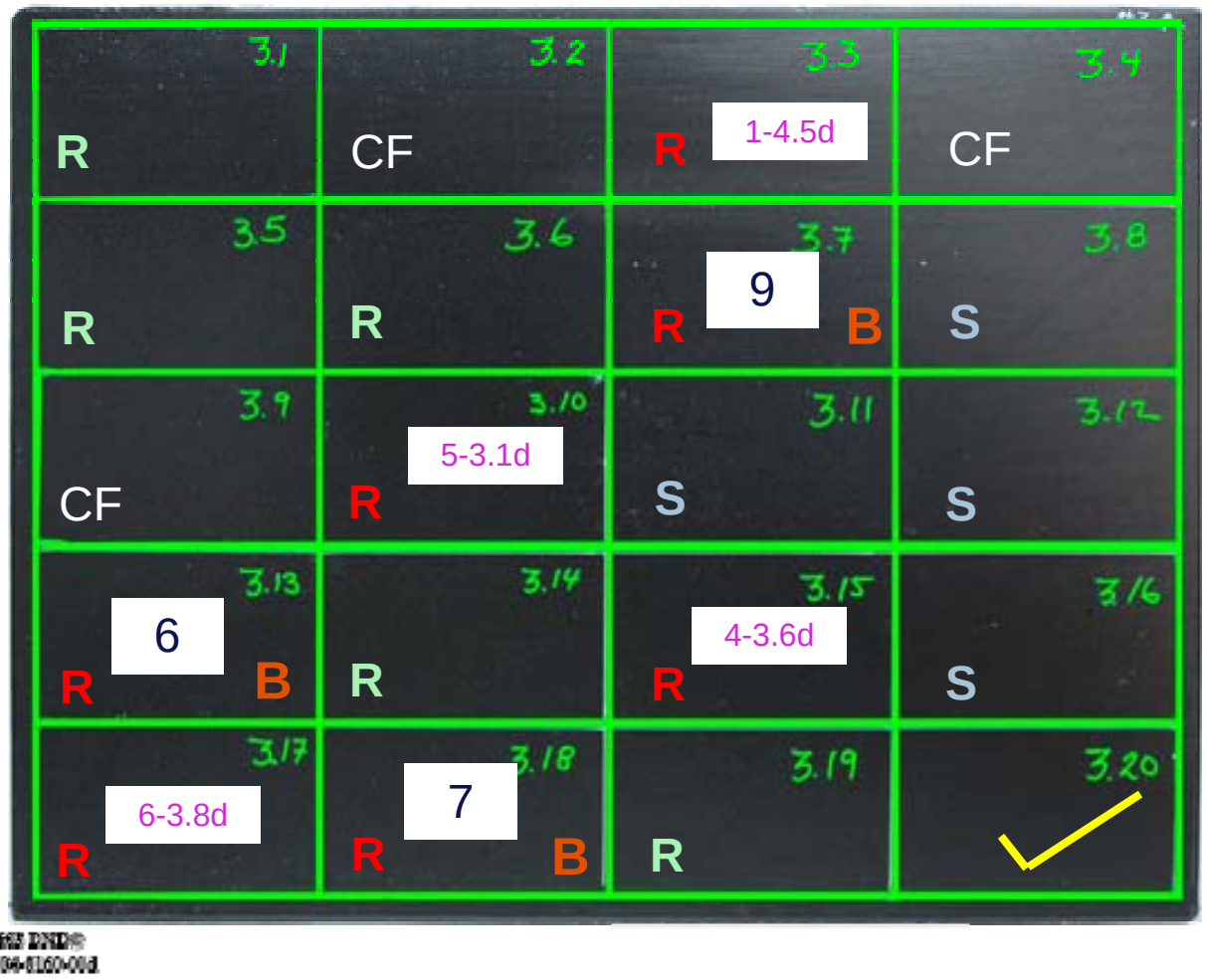

	Successful injection
	Failed injection
	Partially Successful injection
S	Spare coupon
B	Baseline coupon
R	RAAF tested
R	RUAG injection test
CF	CF injection test

As manufactured Panel 3 with coupon locations identified. Numbers in white boxes represent baseline, bold black numeral, damaged, pink numeral with damage diameter and repaired test specimens, blue numeral with repaired damage diameter in inches. Numbers represent the fatigue resistance from worst (1) to best (7, 8 &9).

DISTRIBUTION LIST

Progress Report on DSTO Activities in Support of CREDP Tasks AF, AH and AI

A. N. Rider and D. Parslow

AUSTRALIA

DEFENCE ORGANISATION	**No. of copies**
Task Sponsor	
ASI-4A	1 Printed, 1 PDF
ASI-4D	1 Printed
S&T Program	
Chief Defence Scientist	1
Deputy Chief Defence Scientist Policy	1
AS Science Corporate Management	1
Director General Science Policy Development	1
Counsellor Defence Science, London	Doc Data Sheet
Scientific Advisor to MRDC, Thailand	Doc Data Sheet
Counsellor Defence Science, Washington	Doc Data Sheet
Scientific Adviser Joint	1
Navy Scientific Adviser	1
Scientific Adviser – Army	1
Air Force Scientific Adviser	1
Scientific Adviser to the DMO	1
Deputy Chief Defence Scientist (P&HS)	Doc Data Sht & Exec Summary
Chief of Air Vehicles Division	Doc Data Sht & Dist List
Research Leader, Aircraft Materials – Richard Chester	1
Task Manager - Chun Wang	1
Author (s): Andrew Rider	1 Printed, 1 PDF
David Parslow	1 Printed
DSTO Library and Archives –	
Library Fishermans Bend	Doc Data Sheet
Library Edinburgh	1 printed
Defence Archives	1 printed
Capability Development Group	
Director General Maritime Development	Doc Data Sheet
Director General Capability and Plans	Doc Data Sheet
Assistant Secretary Investment Analysis	Doc Data Sheet
Director Capability Plans and Programming	Doc Data Sheet

Chief Information Officer Group

Head Information Capability Management Division	Doc Data Sheet
Director General Australian Defence Simulation Office	Doc Data Sheet
AS Information Strategy and Futures	Doc Data Sheet
Director General Information Services	Doc Data Sheet

Strategy Executive

Assistant Secretary Strategic Planning	Doc Data Sheet
Assistant Secretary International and Domestic Security Policy	Doc Data Sheet

Navy

Maritime Operational Analysis Centre, Building 89/90 Garden Island Sydney NSW Deputy Director (Operations) Deputy Director (Analysis)	Doc Data Sht & Dist List
Director General Navy Capability, Performance and Plans, Navy Headquarters	Doc Data Sheet
Director General Navy Strategic Policy and Futures, Navy Headquarters	Doc Data Sheet

Air Force

SO (Science) - Headquarters Air Combat Group, RAAF Base, Williamtown NSW 2314	Doc Data Sht & Exec Summary
Staff Officer Science Surveillance and Response Group	Doc Data Sht & Exec Summary

Army

Australian National Coordination Officer ABCA (AS NCO ABCA)	Doc Data Sheet
Land Warfare Development Centre, Puckapunyal	Doc Data Sheet
J86 (TCS GROUP), DJFHQ	Doc Data Sheet
SO (Science) - Land Headquarters (LHQ), Victoria Barracks NSW	Doc Data Sht & Exec Summary
SO (Science) - Special Operations Command (SOCOMD), R5-SB-15, Russell Offices, Canberra	Doc Data Sht & Exec Summary & Dist List
SO (Science), Deployable Joint Force Headquarters (DJFHQ) (L), Enoggera QLD	Doc Data Sheet

Joint Operations Command

Director General Joint Operations	Doc Data Sheet
Chief of Staff Headquarters Joint Operations Command	Doc Data Sheet
Commandant ADF Warfare Centre	Doc Data Sheet
Director General Strategic Logistics	Doc Data Sheet

Intelligence and Security Group

Assistant Secretary Concepts, Capability and Resources	1
DGSTA, Defence Intelligence Organisation	1 Printed
Manager, Information Centre, Defence Intelligence Organisation	1
Director Advanced Capabilities, DIGO	Doc Data Sheet

Defence Materiel Organisation

Deputy CEO	Doc Data Sheet
Head Aerospace Systems Division	Doc Data Sheet
Head Maritime Systems Division	Doc Data Sheet
Program Manager Air Warfare Destroyer	Doc Data Sheet
Guided Weapon & Explosive Ordnance Branch (GWEO)	Doc Data Sheet
CDR Joint Logistics Command	Doc Data Sheet

OTHER ORGANISATIONS

National Library of Australia	1
NASA (Canberra)	1

UNIVERSITIES AND COLLEGES

Australian Defence Force Academy	
Library	1
Head of Aerospace and Mechanical Engineering	1
Hargrave Library, Monash University	Doc Data Sheet

OUTSIDE AUSTRALIA

INTERNATIONAL DEFENCE INFORMATION CENTRES

US Defense Technical Information Center	1
UK Dstl Knowledge Services	1
Canada Defence Research Directorate R&D Knowledge & Information Management (DRDKIM)	1
NZ Defence Information Centre	1

ABSTRACTING AND INFORMATION ORGANISATIONS

Library, Chemical Abstracts Reference Servie	1
Engineering Societies Library, US	1
Materials Information, Cambridge Scientific Abstracts, US	1
Documents Librarian, The Center for Research Libraries, US	1

SPARES	5 Printed

Total number of copies: 39 Printed: 12 PDF: 27

DEFENCE SCIENCE AND TECHNOLOGY ORGANISATION
DOCUMENT CONTROL DATA

1. PRIVACY MARKING/CAVEAT (OF DOCUMENT)

2. TITLE

Progress Report on Activities in Support of Composite Repair Engineering Development Program Tasks AF, AH and AI

3. SECURITY CLASSIFICATION (FOR UNCLASSIFIED REPORTS THAT ARE LIMITED RELEASE USE (L) NEXT TO DOCUMENT CLASSIFICATION)

Document	(U)
Title	(U)
Abstract	(U)

4. AUTHOR(S)

A. N. Rider and D. Parslow

5. CORPORATE AUTHOR

DSTO Defence Science and Technology Organisation
506 Lorimer St
Fishermans Bend Victoria 3207 Australia

6a. DSTO NUMBER	6b. AR NUMBER	6c. TYPE OF REPORT	7. DOCUMENT DATE
DSTO-TR-1932	AR-013-778	Technical Report	November 2006

8. FILE NUMBER	9. TASK NUMBER	10. TASK SPONSOR	11. NO. OF PAGES	12. NO. OF REFERENCES
2006/1163454/1	AIR 04/241	DSTO	56	8

13. URL on the World Wide Web

http://www.dsto.defence.gov.au/corporate/reports/DSTO-TR-1932.pdf

14. RELEASE AUTHORITY

Chief, Air Vehicles Division

15. SECONDARY RELEASE STATEMENT OF THIS DOCUMENT

Approved for public release

OVERSEAS ENQUIRIES OUTSIDE STATED LIMITATIONS SHOULD BE REFERRED THROUGH DOCUMENT EXCHANGE, PO BOX 1500, EDINBURGH, SA 5111

16. DELIBERATE ANNOUNCEMENT

No Limitations

17. CITATION IN OTHER DOCUMENTS Yes

18. DSTO RESEARCH LIBRARY THESAURUS http://web-vic.dsto.defence.gov.au/workareas/library/resources/dsto_thesaurus.htm

Adhesive bonding, bonded repairs, surface treatment

19. ABSTRACT

Research has been undertaken to support the Royal Australian Air Force's commitments to the F/A-18 Composite Repair Engineering Development Program (CREDP). This report details work that has examined the effectiveness of surface treatments for adhesive bonding to aluminium, titanium and stainless steel (Tasks AF and AH) and the benefit of resin injection repairs to damaged composite laminates to restore fatigue strength (Task AI). The studies showed that bonding to high modulus metals using current and new generation surface treatment processes does not appear to be as effective as on aluminium alloys. Resin injection repairs to damaged composite laminates shows some measurable improvements over unrepaired laminates when tested in compression-compression fatigue.